Framed link presentations of 3-manifolds by an $O(n^2)$ algorithm, III: geometric complex $\mathcal{H}_n^\star$ embedded into $\mathbb{R}^3$ *

Sóstenes Lins and Ricardo Machado

April 30, 2013

Abstract

In this final part of a 3-part paper we introduce the pair of "wings" of the abstract PL-colored complexes $\mathcal{H}_m^\star$, described in the second paper. The wings, via a weight enhanced Tutte's barycentric embedding of a planar map, produce the unexpected reformutation of a 3-dimensionl problem into a 2-dimensional one. The total number of edges in each one of the pair of final wings is less than $8n-5$. Tutte's method is applied $O(n)$ times to each one of the 2 wings in the final pair to assure rectilinearity of the embeddings of the planar maps, which include the final wings. A cone construction over the final wings provides a PL-complex $\mathcal{H}_1^\diamond$, which contain the set of 0-simplices $\{a_1, a_2, \ldots, a_f\} \cup \{b_1, b_2, \ldots, b_g\}$ (as defined in the second part of the article) properly fixed in $\mathbb{R}^3$. The other 0-simplices are obtained by bisections of segments linking previously defined points. This implies that $\mathcal{H}_n$ is PL-embedded into $\mathbb{R}^3$. We then conclude the surgery description of the 3-manifold induced by the gem with its resolution by defining some disjoint cylinders contained in $\mathcal{H}_n^\star$, directly from the hinges (dual of the twistors of the resolution), in a 1-1 correspondence. The medial curves of the cylinders define the link we seek. The framing of a medial curve is the linking number of the boundary components of the corresponding cylinder. The analysis of the whole proccess shows that the memory and time requirement to complete the algorithm is $O(n^2)$. Data for the Weber-Seifert 3-manifold, which answers Jeffrey Weeks's question is given in the appendix. It consists of a link with 142 crossings but it admits simplifications.

1 Wings as seeds for obtaining the dual PL-complex $\mathcal{H}_n^\star$

This is the third of 3 closely related articles. References for the companion papers are [6] and [7].

Let Π_ℓ (Π_r) be the half plane limited by the z-axis which contains $a_1 = z_0 z_2/2$ ($b_1 = z_1 z_2/2$). The construction of the wings and nervures of the next section are exemplified in Figs. 19 to 29.

1.1 Wings: reformulating a difficult 3D-problem into an easy planar one

At some point in our research it became evident that what was needed to obtain the PL-complex $\mathcal{H}_n^\star$ was a proper embedding into $\mathbb{R}^3$ of the set of 0-simplices $\{a_1, a_2, \ldots, a_f\} \cup \{b_1, b_2, \ldots, b_g\}$. The other 0-simplices are obtained by bisections of segments linking previously defined points. It came as a surprise to discover that this apparently difficult 3D problem was reformulated as a plane problem for which we had at hand an easy solution, namely Tutte's barycentric method.

We construct a sequence of pairs of plane graphs $\{\{\mathcal{W}_1^\ell, \mathcal{W}_1^r\}, \{\mathcal{W}_2^\ell, \mathcal{W}_2^r\}, \ldots, \{\mathcal{W}_n^\ell, \mathcal{W}_n^r\}\}$. The m-th such pair constitutes the *left* and *right wings* of the colored 2-complex $\mathcal{H}_m^\star$. The left wings are embedded into Π_ℓ and the right wings are embedded into Π_r. We define $\mathcal{W}_1^\ell$ as the set of $2n$ straight line segments $a_1 z_3^1, a_1 z_3^2, \ldots, a_1 z_3^{2n} \subseteq \Pi_\ell$, and $\mathcal{W}_1^\ell$ as the set of $2n$ straight line segments $b_1 z_3^1, b_1 z_3^2, \ldots, b_1 z_3^{2n} \subseteq \Pi_r$. The *outer triangular region of the left wings* is the plane region spanned by a_1, z_3^1, z_3^{2n}. The *outer triangular region of the right wings* is the plane region spanned by b_1, z_3^1, z_3^{2n}. The passage from $\{\mathcal{W}_{m-1}^\ell, \mathcal{W}_{m-1}^r\}$ to $\{\mathcal{W}_m^\ell, \mathcal{W}_m^r\}$ in the $(m-1)$-th *bp*-move, which we call a *wbp-move*, corresponds in $(\mathcal{H}_{m-1}, \mathcal{H}_m)$ to either a 0-flip that subdivides a 13-gon into two (case where the tail of the balloon is of color 0) or else to a 1-flip that subdivides a 03-gon into two (case where the tail of the balloon's is of color 1). At this point, we need to define a tree called the *nervure of a wing*. This is done inductively. The first ones, $\mathcal{W}_1^\ell$ and $\mathcal{W}_1^r$ have, respectively the degenerated trees formed by single points

*2010 Mathematics Subject Classification: 57M25 and 57Q15 (primary), 57M27 and 57M15 (secondary)

a_1 and b_1 as their nervures. In the unique wing that changes with the *bp*-move, a vertex x_ℓ corresponding to either a 13-gon or else to a 03-gon (in a way to be made clear in the poof of Lemma 1.1). The intersection of the balloon's head and its tail in $\mathcal{H}^\star_m$ is a PL1-face formed by two simplices meeting at a point a_p (if the tail of the balloon is of color 1) or b_q, if it is of color 0. Along the process we define the following auxiliary functions, with arguments $1 \leq m \leq n-1$: $c(m), u(m), v(m), r(m), s(m), \ell_a(m), \ell_b(m), t_a(m), t_b(m)$. The color of the m-th balloon's tail is denoted by $c(m) \in \{0,1\}$. Let $u(m), v(m)$ be the odd and even indices of the m-th balloon's head $\nabla_{u(m)} \cup \nabla_{v(m)}$. Let $r(m), s(m)$ be the odd and even indices of the m-th balloon's tail given by the PL2$_{c(m)}$-face $\subseteq \nabla_{r(m)} \cap \nabla_{s(m)}$. The positive integers $\ell_a(m)$ and $\ell_b(m)$ are the last a- and b-indices in left m-th wing and right m-th wing, respectively. Indices p or q in the m-th *bp*-move satisfy $p = t_a(m)$ or $q = t_b(m)$. In the passage $\mathcal{H}^\star_m$ to $\mathcal{H}^*_{m+1}$ either vertex a_p is replaced by $a_{p'}, A_p, a_{p''}$, where $p' = \ell_a(m)+1$ and $p'' = \ell_a(m)+2$ or else b_q is replaced by $b_{q'}, B_p, b_{q''}$, where $q' = \ell_b(m)+1$ and $q'' = \ell_b(m)+2$, depending on the color of the balloon's tail. In the first case, we add two new edges $a_{p'}A_p$ and $a_{p''}A_p$ to the nervure, in the second case, we add the edges $b_{q'}B_p$ and $b_{q''}B_q$ to the nervure. In both cases, $p'' = p'+1$ or $q'' = q'+1$. In the pictures the edges of the nervure are thicker than the ones in the respective wing. For $1 \leq m \leq n$, and $h \in \{\ell, r\}$, the nervure of $\mathcal{W}^h_m$, denoted $\mathcal{N}^h_m$, is a spanning tree of the graph $\mathcal{W}^h_m \cup \mathcal{N}^h_m \backslash Z$, where $Z = \{z^j_3 \mid j \in \{1, \ldots, 2n\}\}$. See Fig. 1, Fig. 2, Fig. 3 and the complete sequence of figures for the r^{24}_5-example, Figs. 19-29. A vertex in the tree $\mathcal{N}^h_m$ is *pendant* if it has degree at most 1.

(1.1) Lemma. *Let $1 \leq m \leq n$. The set of pendant vertices of $\mathcal{N}^\ell_m$ is in 1-1 correspondence with the set of 13-gons of $\mathcal{H}_m$. The set of pendant vertices in $\mathcal{N}^r_m$ is in 1-1 correspondence with the 03-gons of $\mathcal{H}_m$.*

Proof. The intersection of the $(m-1)$-th balloon's head and tail is a PL1-face with two 1-simplices. Their intersection is a point in Π_h. The PL1-face dualy corresponds to a 13-gon (resp. 03-gon) in $\mathcal{H}_{m-1}$ if $h = \ell$ ($h = r$). After the 0-flip (resp. 1-flip) that produces $\mathcal{H}_m$ the PL1-face is splitted into two, in a conformal way with the passage from $\mathcal{W}^h_{m-1} \cup \mathcal{N}^h_{m-1}$ to $\mathcal{W}^h_m \cup \mathcal{N}^h_m$. Given this interpretation the Lemma is easily established by induction. □

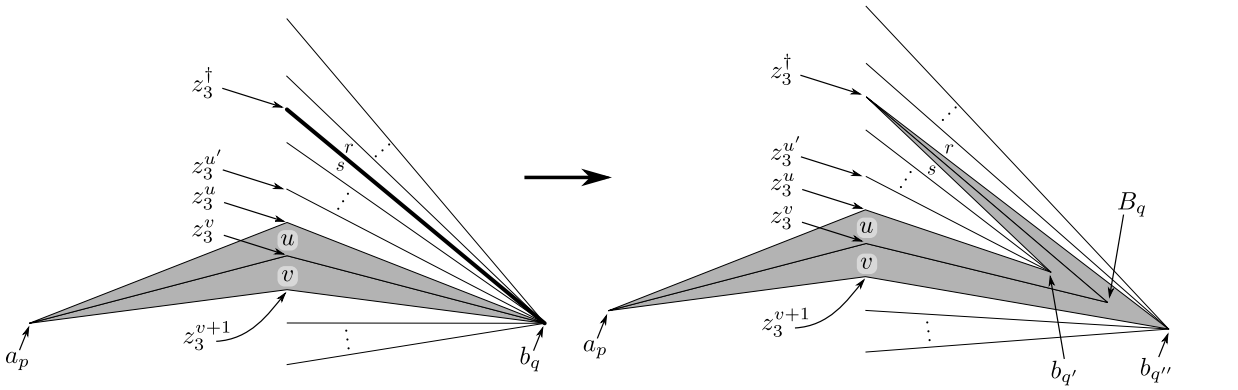

Figure 1: *wbp*-move: balloon's head section is painted in gray, and the part of balloon's tail that is intersecting the appropriate semi-plane is depicted as a *thick edge*.

A graph is *rectilinearly embedded into* $\mathbb{R}^3$ if the images of their edges are straight line segments. It is a straightforward application of Tutte's barycentric method [11], [1] to obtain a rectilinear embedding of $\mathcal{W}^h_n \cup \mathcal{N}^h_n$ which fixes the vertices in the boundary of the outer triangular region of Π_h, $h \in \{\ell, r\}$. Tutte's method has an intrinsic connection with the Laplacian of graphs, see [2]. We rotate $\Pi \in \{\Pi_\ell, \Pi_r\}$ so that it becomes the xz-plane. After having the planar coordinates Π_h is rotated back to its initial position and we have the $\mathcal{W}^h_n \cup \mathcal{N}^h_n$ rectilinearly embedded into $\mathbb{R}^3$. Tutte's method becomes very efficient because of Lemma 1.2.

Tutte's method suffers of the clustering problem where vertices accumulate in some small regions. Even though theoretically this is not needed, we present a heuristic of attaching weights to the edges to improve the result. An edge with weight $k \in \mathbb{N}$ behaves as k parallel edges. We define the weights for the edges of the wings as 1. If the edge is in the nervure, to calculate the weight, we use the whole wing. Start defining these weights as 0, so from leaves to root, define the weight of an edge as the weight of the vertex incident to it and closer to the leaves minus 1, Fig. 4. In Fig. 5 we compare the two results, without and with weights given by three times the weights in the nervure of Fig. 4, for obtaining the final left wing of the r^{24}_5-example.

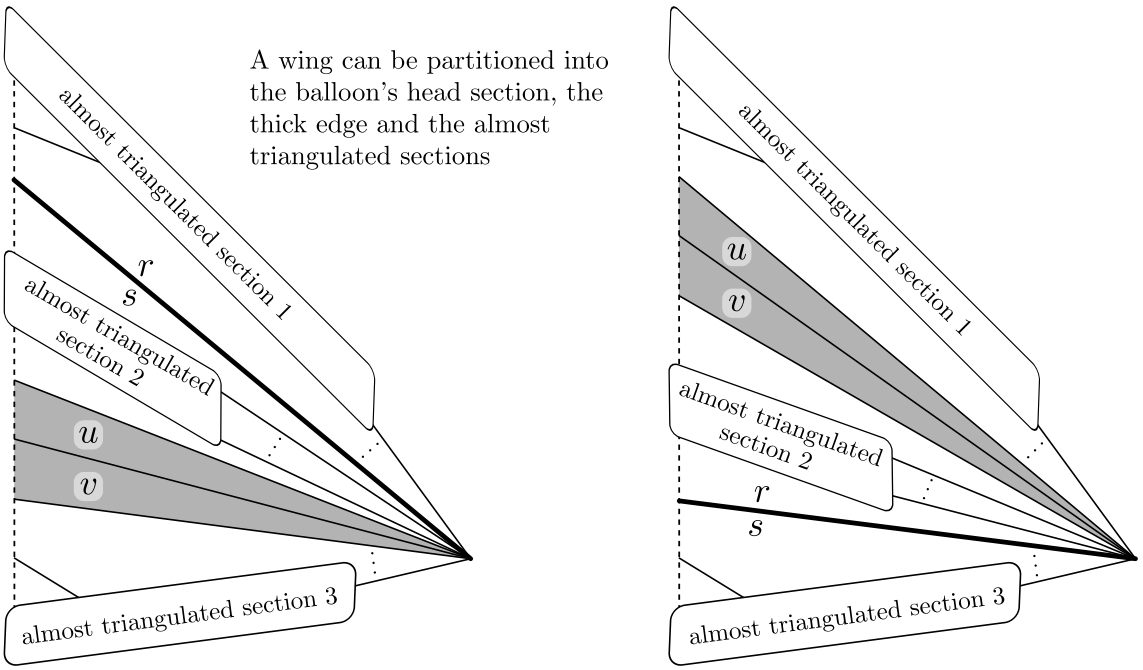

Figure 2: Given a half-wing and a balloon it can be partitioned into the balloon's head section, thick edge and some *almost triangulated* sections.

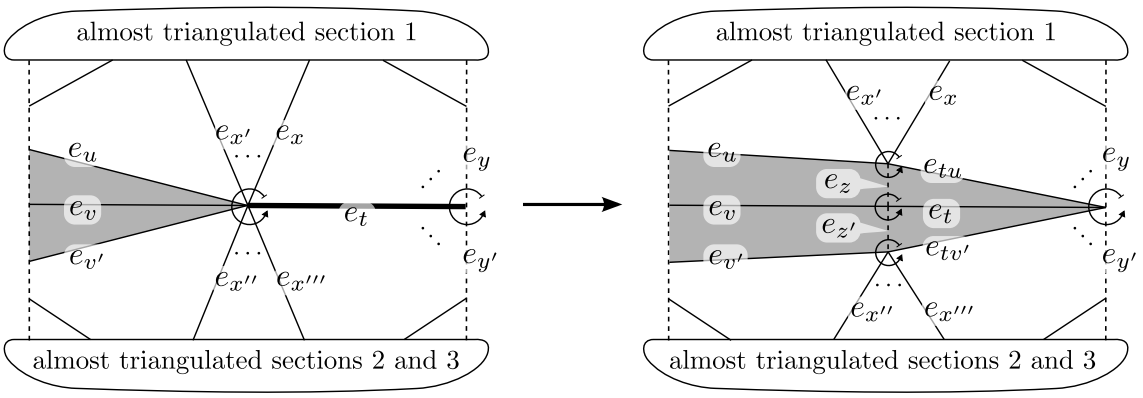

Figure 3: The *star* of a vertex of a graph embedded in a surface is the counterclockwise cyclic sequence of edges incident to the vertex (such an ordering is induced by the surface). The set of stars is called a *rotation* and has the characterizing property that each edge appears twice. The general case of changing rotation when going from $\mathcal{W}_{\ell-1} \cup \mathcal{N}_{\ell-1}$ to $\mathcal{W}_\ell \cup \mathcal{N}_\ell$ is depicted above. The rotation completely specifies the topological embedding.

Tutte's method is applied twice: to plane graphs $\mathcal{W}_n^\ell \cup \mathcal{N}_n^\ell$ and to $\mathcal{W}_n^r \cup \mathcal{N}_n^r$. In each application we use $O(n)$ iterations to solve a linear system in $\mathbb{C}$. This is theoretically sufficient to achive rectilineatiry (which nevertheless can be verified). As each one of the plane graphs has less than $6n - 4$ edges by Lemma 1.2, the total time to obtain $\mathcal{W}_n^\ell \cup \mathcal{W}_n^r$ embedded into $\Pi_\ell \cup \Pi_r$ is $O(n^2)$.

(1.2) Lemma. *The number of edges of* $\mathcal{W}_n^h \cup \mathcal{N}_n^h$, $h \in \{\ell, r\}$ *is at most* $6n-4$.

Proof. The number of 1-simplices in the left wing and in the right wing of the initial complex in the sequence are both $2n$. At each one of the $n-1$ *bp*-moves we add 4 edges either to the left or to the right wing with its nervure. Thus each one of the final left and right wings with nervures has at most $6n-4$ edges. □

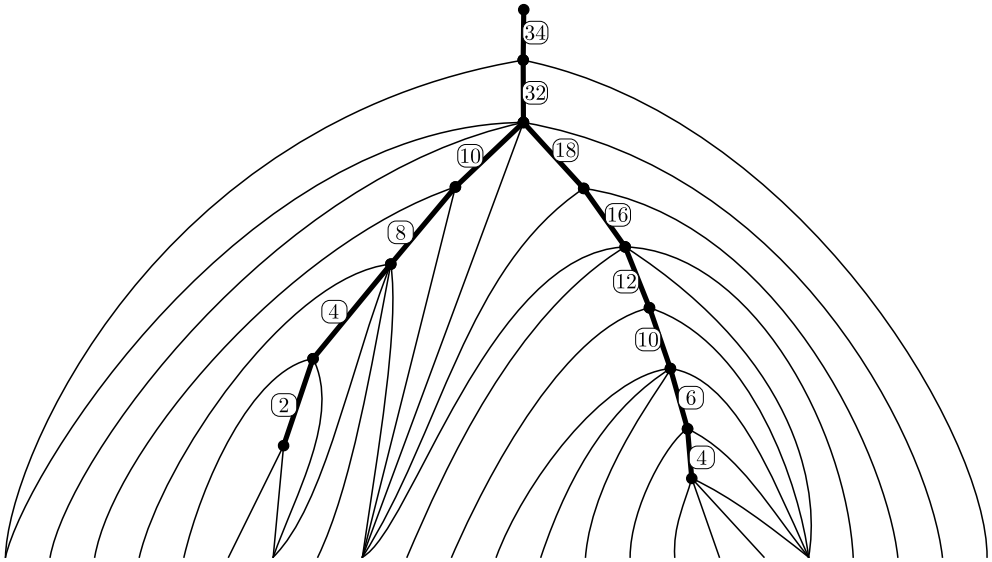

Figure 4: Computing the weights for Tutte's barycentric method via the wing nervure.

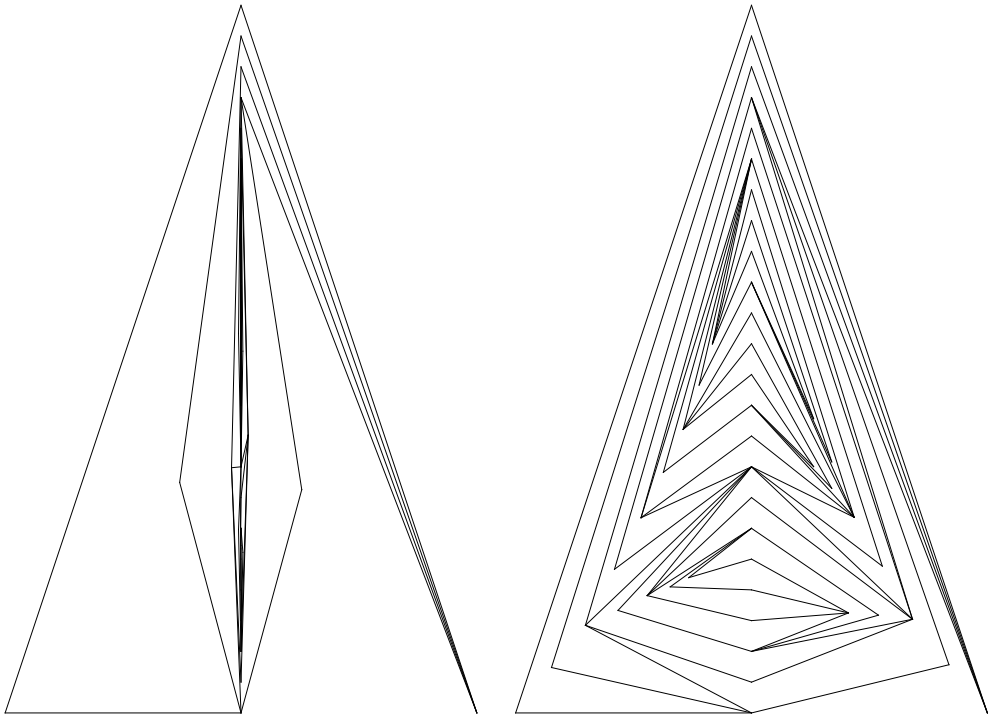

Figure 5: Tutte's embbeding without and with the weights (final pair of wings without nervure for the r_5^{24}-example).

2 Defining the PL-embedding $\mathcal{H}_1^\diamond$

Let $\mathcal{L}_{i+1}^\star$ be a subset of the pillow $\mathcal{P}_{i+1}^\star$, formed by the part that comes from the tail of the balloon after the i-th *bp*-move is applied, see Fig. 6.

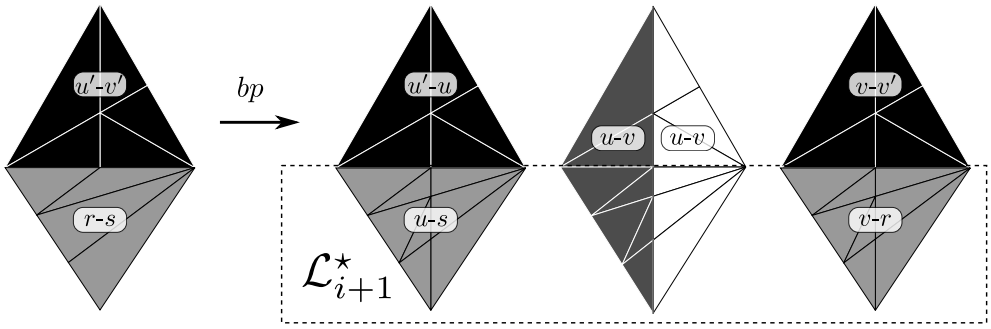

Figure 6: The set $\mathcal{L}_{i+1}^\star$.

Let $\{x\} \cup Y \subseteq \mathbb{R}^N$, for $1 \leq N \in \mathbb{N}$. The *cone* [10] with vertex x and base Y, denoted $x * Y \subseteq \mathbb{R}^N$, is the union of Y with all line segments which link x to $y \in Y$.

Now we define a PL-complex $\mathcal{H}_1^\diamond$ explicitly embedded into $\mathbb{R}^3$. We use the (rectilinearly embedded into $\Pi_\ell \cup \Pi_r$) final wings and the cone contruction to get the $\mathcal{H}_1^\diamond$. To this end, select a distinguished representative of the edges of $\mathcal{W}_n^\ell$ (resp. $\mathcal{W}_n^r$) incident to z_3^j in the following way: if there is just one edge, choose it, otherwise the representative is the edge whose other end has the smallest indexed upper case label. Let R denote the set of representatives.

For each $e \in R$ add the two 2-simplices $z_0 * e$ and $z_2 * e$ (resp. the two 2-simplices $z_1 * e$ and $z_2 * e$) to $\mathcal{H}_1^\diamond$. To complete $\mathcal{H}_1^\diamond$ add the 2-simplices $\{z_3^j z_1 z_0 \mid j = 1, \ldots, 2n\}$. In Fig. 7 the solid lines (the edges of R) and the dashed edges are part of $\mathcal{L}_i^\star$, and are treated in next section.

(2.1) Proposition. *If $\mathcal{W}_m^h$ is embedded rectilinearly in Π_h, $h \in \{\ell, r\}$, then the pair of embeddings can be extended to an embedding of $\mathcal{H}_1^\diamond$ into $\mathbb{R}^3$, via the cone construction.*

Proof. Straighforward from the simple geometry of the situation. □

3 Blowing up the tails and constructing $\mathcal{H}_2^\diamond, \mathcal{H}_3^\diamond, \ldots, \mathcal{H}_n^\diamond = \mathcal{H}_n^\star$

The process of replacing the embedded tail of a balloon by the corresponding trio of PL2-faces in the pillow is denominated *the blowing up of the balloon's tail.*

(3.1) Theorem. *There is an $O(n)$-algorithm for blowing up a single balloon's tail. Thus finding $\mathcal{H}_n^\star$ take, $O(n^2)$ steps.*

Proof. $\mathcal{H}_{i+1}^\diamond$ is the union of $\mathcal{H}_i^\diamond$ with $\mathcal{L}_{i+1}^\star$ and an *ϵ-change* in some PL3-faces, if the rank of the type of balloon's tail of the i-th *bp*-move has rank greater than 1 (we call ϵ-change because this change is small, as described below). At the same time we update the colors of the middle layer to match the colors of the i-th pillow in the sequence of *bp*-moves.

Now we describe how to embed each kind of $\mathcal{L}_i^\star$ (explaining how to ϵ-change some PL3-faces, to get space for $E\mathcal{L}_i^\star$).

If the balloon's tail is of type P_1 (the case B_1 is analogous). Make two copies of P_1, resulting in three P_1, but change the color of the one which will be in the middle, and define the 0-simplices like in Fig. 8.

If the balloon's tail is of type B_i, $i > 1$ (the case P_i is analogous). Make two copies of B_i, refine the copies and the original, resulting in three B_i', but change the color of the one which will be in the middle, and define the 0-simplices like in Fig. 9.

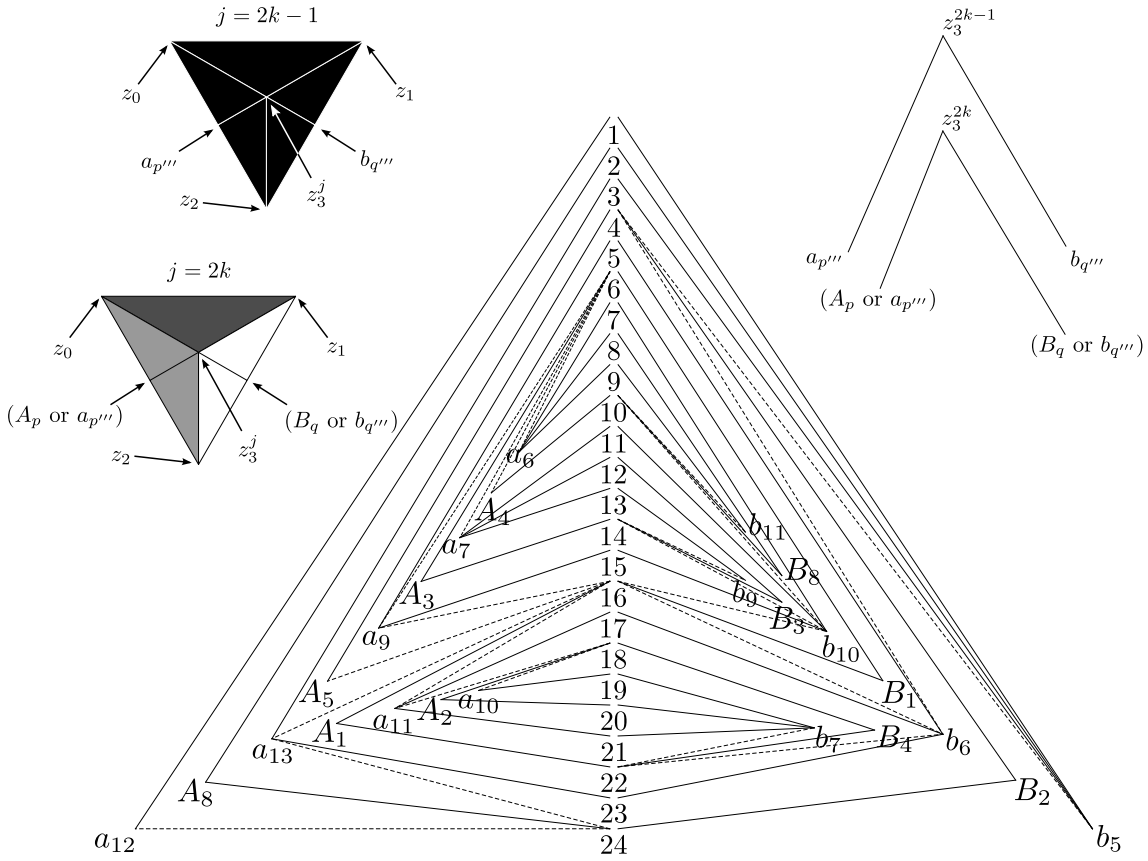

Figure 7: We use the cone construction with the solid lines to obtain $\mathcal{H}_1^\diamond$. Then we use the dashed lines to obtain the information of $z_3^\dagger$ and $a_{p'}, A_p, a_{p''}$ or $b_{q'}, B_q, b_{q''}$ latter when obtaining $\mathcal{L}_i^\star$. Also, we have $p''' \in \{p', p''\}$ and $q''' \in \{q', q''\}$.

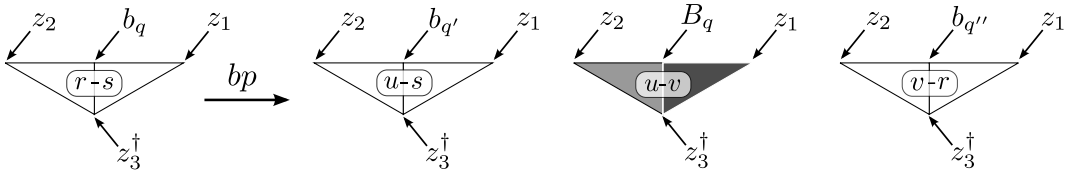

Figure 8: Embedding the part of the pillow corresponding to the tail of the balloon: case P_1 of the tail.

The images χ_j we already know from previous *bp*-move, now we need to define all the images α_j, β_j and γ_j. Let β_j be $\frac{z_2+\chi_{j+1}}{2}$ for each $j = 1, \ldots, i$. As the images α_j and γ_j can be defined in analogus way, we just explain how to define each α_j. We know that each α_j is in the PL3-face ∇_r. To define each α_j we need to reduce the PL3-face ∇_r in order to get enough space for the PL2-faces of color 0 and 2 of the PL3-faces ∇_u and ∇_v. Consider the PL3-face ∇_r, each β_j is already defined, so define each ζ_j as $\frac{z_2+\omega_{j+1}}{2}$, where ω_k is previously defined, see Fig. 10. Define α_j as $\frac{\zeta_j+\beta_j}{2}$.

The last case is when balloon's tail is refined, that means it is of type P_i' or B_i', $i > 1$. We treat the case B_i', see Fig. 11. All the 0-simplices β_j are already defined, we need to define each α_j and each γ_j. Observe that here $r \neq s-1$ and the definitions of α_j and γ_j are not analogous.

In this case, we need to reduce the PL3-faces ∇_r and ∇_s to create enough space to build PL2-faces 0- and 2-colored. To define 0-simplices α_j and γ_j, one of these cases is analogous to the case not refined, but the other we describe here. (∇_r is in the new case is the rank of PL2_0-face is equals to the rank of the PL2_1-face plus 2, if its not true, the new case is in the PL3-face ∇_v). Suppose that the new case is in the PL3-face, ∇_r. To

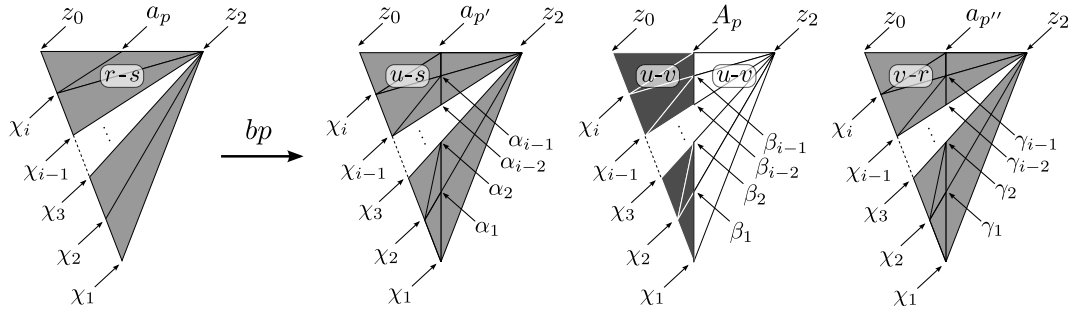

Figure 9: Embedding the part of the pillow corresponding to the tail of the balloon: case B_i of the tail.

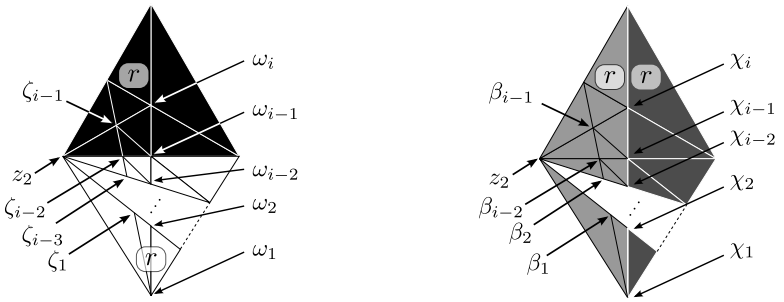

Figure 10: Using the PL3-face corresponding to r to define the α_j as $\frac{\zeta_j+\beta_j}{2}$.

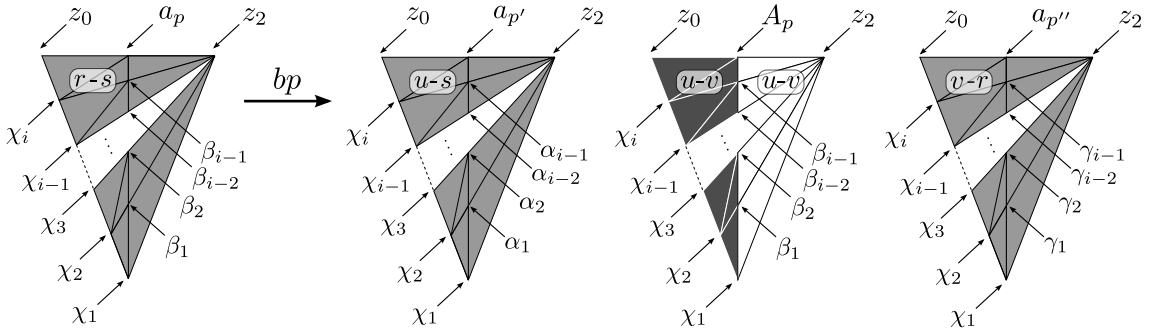

Figure 11: Embedding the part of the pillow corresponding to the tail of the balloon: case B'_i of the tail.

define α_j, suppose that the PL2$_0$-face of this PL3-face is not refined, see Fig. 12. Define each α_j as the middle point between β_j and ω_j.

Consider the case that the PL2$_0$-face, of the PL3-face ∇_r, is refined see Fig. 13. This is a final subtlety which is treated with the *bump*. This is characterized by a non-convex pentagon shown in the bottom part of Fig. 13. Let ν_j be $\frac{z_2+\omega_j}{2}$ and α_j as $\frac{\beta_{j-1}+\nu_j}{2}$, for $j = 1, \ldots, i-1$. Observe that if we define α_j as if the PL2$_0$-face where not refined, some 1-simplices may cross. □

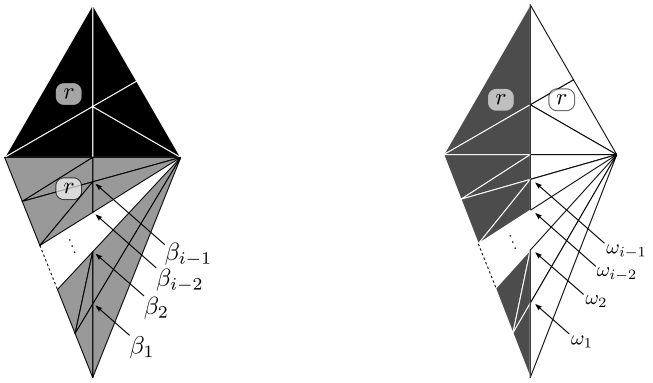

Figure 12: Using the PL3-face ∇_r to define α_j as $\frac{\omega_j+\beta_j}{2}$.

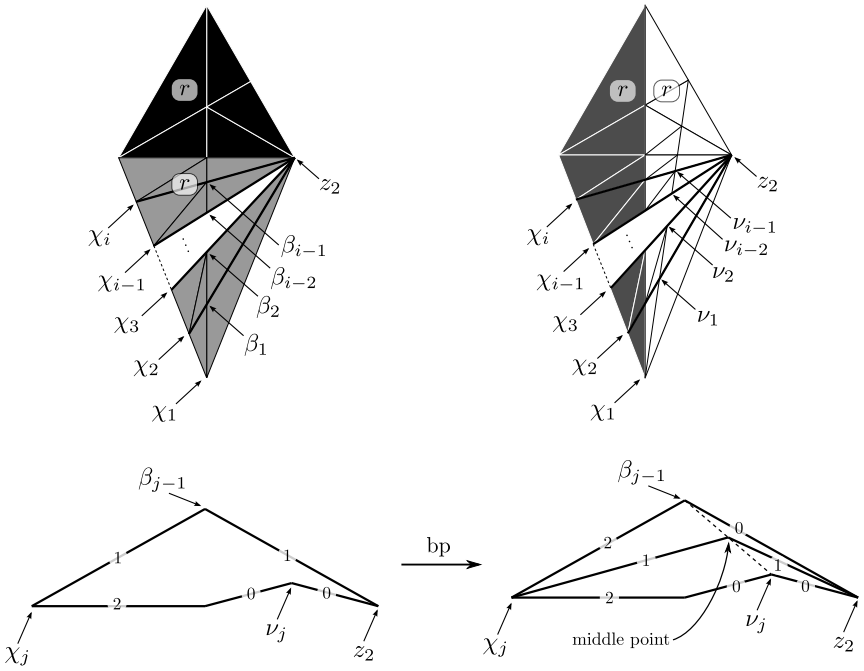

Figure 13: The bump: a final subtlety and how to deal with it.

4 Obtaining the framed Link

Given $\mathcal{H}_n^\star$ into $\mathbb{R}^3$ we obtain the k-component framed link (corresponding to the k twistors) as a set of PL-triangulated k cylinders in the 2-skeleton of $\mathcal{H}_n^\star$, named $\mathcal{C}_1, \mathcal{C}_2, \ldots, \mathcal{C}_k$. Observe that at this stage every 0-simplex of $\bigcup_{j=1}^k \mathcal{C}_j$ has a 3-D coordinate attached to it. These cylinders are parametrized as k pairs of isometric rectangles (forming a strip) as in Fig. 14. We draw k straight horizontal lines at different heights of the rectangles, in the example, lines $c_1 - c_1$, $c_2 - c_2$ and $c_3 - c_3$. These lines are mapped into polygons in $\mathbb{R}^3$ which are PL-closed curves. The data we need is $\bigcup_{j=1}^k \mathcal{C}_j \subset \mathcal{H}_n^\star$ and we can discard the rest of $\mathcal{H}_n^\star$. The link that we seek is $\bigcup_{j=1}^k c_j$ with framing ℓ_j, where ℓ_j is given by the linking number of the two components of $\mathcal{C}_j$ oriented in the same (arbitrary) direction. We briefly review the definition of linking number [3]. Consider two distinct components K_1 and K_2 of an oriented link projected into the plane so that the crossings are transversal (no tangency) and that there are no triple points. The projection is also *decorated* in the sense that at each crossing the upper and the lower strands are given, usually, by omitting a small segment of the lower strand. The *linking number* of $\{K_1, K_2\}$ is half of the algebraic sum of the signs of the crossings between K_1 and K_2, oriented in the same direction. If G is a gem, $|G|$ means the 3-manifold induced by G. The link projection given in Fig. 15 which

induce $|r_5^{24}|$ has its three linking numbers -3.

(4.1) Proposition. *The number of 1-simplices in $\bigcup_{j=1}^{k} c_j$ is at most $12n^2$, where $2n$ is the number of vertices of the input gem.*

Proof. A c_j crosses one PL2$_m$-face, for $m \in \{0,1,2,3\}$. It is easy to verify that the maximum number of 2-simplices in B_i' or P_i' is $3i-1$ and this number exceeds similar numbers for B_i, P_i, R_i^b and R_i^p, for $i \geq 1$. The maximum i is $2n-1$, so the maximum number of 2-simplices 0-, 1- and 2-colored in one PL2-face of the final complex is $6n-4$. Each 1-simplex of c_j crosses at most once each 2-simplex. Therefore, the number of 1-simpices crossing a 2-simplex 0-, 1- and 2-colored is at most $12n-8$. A c_j crosses at most four 2-simplices 3-colored. The result follows because n is an upper bound for k, number of components. Just note that a component in the link is in 1-1 correspondence with the twistors of the original gem and a twistor is formed by 2 vertices. This proof is partially ilustrated in Fig. 14. The illustration is not faithful because we can replace the strips at the right by their bottom parts, getting simpler cylinders homotopic to the ones illustrated. □

Each cylinder is formed by two strips. Each strip by two adequate pairs of two PL2-faces in the boundary of the PL3-faces in the hinge. In the way depicted we have one PL3-face of each color c, $c = 0,1,2,3$. The number of crossings of the curves c_j, $j = 1,2,3$ coincides with the number of 1-simplices (or 0-simplices) of $\bigcup_{j=1}^{3} \mathcal{C}_j$. To decrease this number we can replace the part of the strip which does not use a PL2$_3$-face by the two complementary PL2$_3$-faces in the corresponding PL3-face. This produces isotopic cylinders, but the number of crossings of the c_j's are smaller. Note that each PL2$_3$-face has just five 2-simplices. In Fig. 14 we depict the situation for the wings arising from r_5^{24} before the 3 replacements.

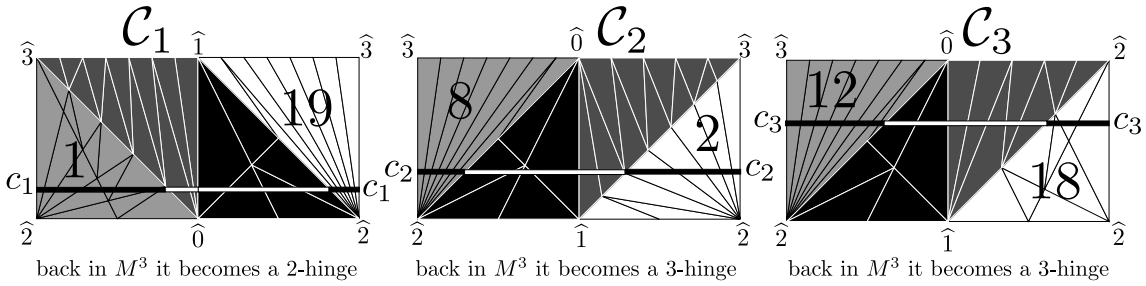

Figure 14: From hinges to cylinders $\mathcal{C}_j$ to curves c_j (example inducing $|r_5^{24}|$).

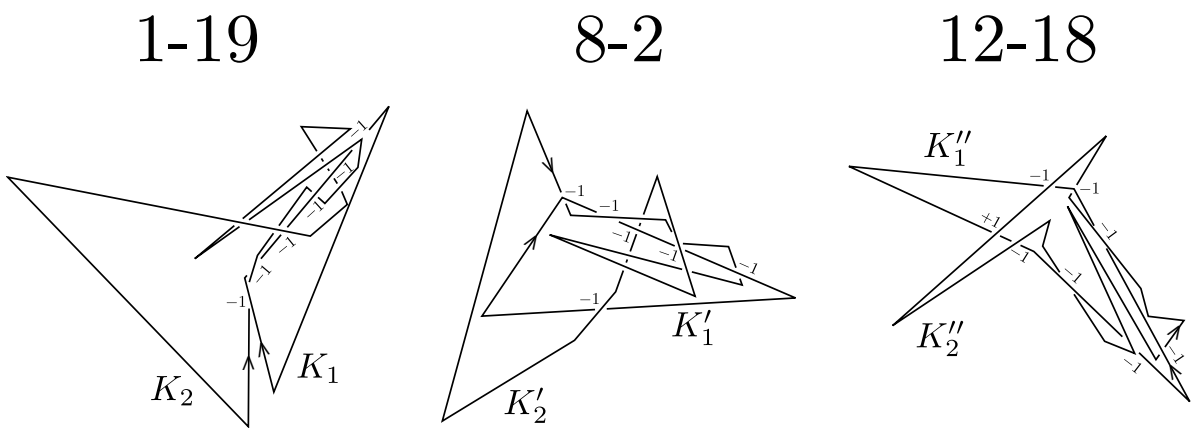

Figure 15: Projection of the algorithm's output, yielding the linking numbers of the boundary components of the embedded cylinders of Fig. 14.

5 Obtaining a Gauss code for the link

At this point, we have the link as a set of cyclic sequences of points in $\mathbb{R}^3$. We also have the framing of each component. Thus the theoretical problem is solved. However, it is convenient to go on getting adequate planar projections to produce planar diagram for the link. We obtain the following Gauss code, ([9], chapter 3 of [5], [8]), where signs mean up (+) and down (−) passages: $((-2,+3,-4,+1),(-5,+6,+2,-1),(-3,+4,-7,-6,+5,+7))$. From this code we get the link planar diagram of Figs. 16. Since we have the framings curls can be removed. An explicit elegant framed link inducing the euclidean 3-manifold $|r_5^{24}|$ was previously unknown. We use Fig. 17 as input for L. Lins's software [4] to obtain the WRT-invariants from $r = 3$ to $r = 20$ for the space $|r_5^{24}|$. We also apply our algorithm for the Weber-Seifert hyperbolic dodecahedron space, obtaining a link with 142 crossings, included in Appendix B.

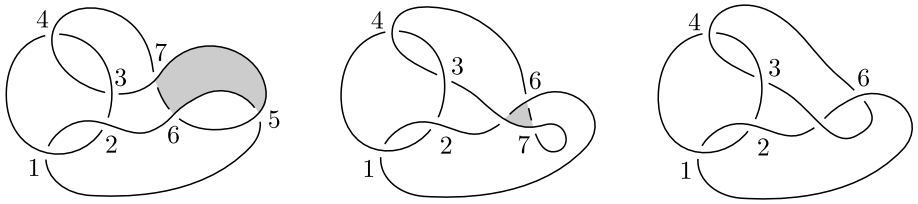

Figure 16: Simplifying the link diagram for $|r_5^{24}|$.

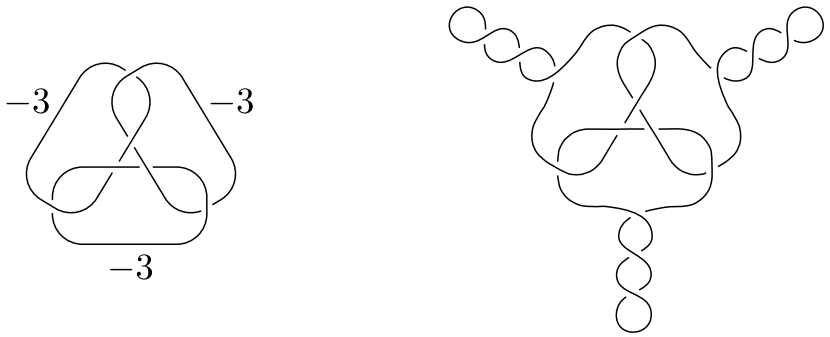

r	WRT-value	Number of states	Time(sec)
3	-1,414214	8	0,0
4	2,000000	48	0,0
5	-2,406004	208	0,0
6	2,886751	703	0,0
7	-3,269578	2008	0,0
8	3,695518	5000	0,0
9	-4,057097	11256	0,1
10	4,447214	23281	0,2
11	-4,790704	45056	0,3
12	5,154701	82352	0,6
13	-5,482825	143624	1,1
14	5,826512	240399	1,8
15	-6,141445	388624	3,0
16	6,468658	609104	4,6
17	-6,772125	929424	7,5
18	7,085570	1384401	10,9
19	-7,378954	2018712	16,5
20	7,680633	2887312	23,3

Figure 17: Framed link, blackboard framed link and WRT-invariants for $|r_5^{24}|$. Data obtained from L. Lins software [4].

(5.1) Algorithm. There exists an $O(n^2)$-algorithm to produce, from a resoluble gem inducing an M^3, a blackboard framed link also inducing M^3.

Proof. We start with a resoluble gem G with $2n$ vertices. Here is the algorithm, justified by the theory previously developed:

- Form decreasing sequence of gems starting with $\mathcal{J}^2$, the J^2-gem associated with the resolution of G performing adequate 0- or 1-flips and finishing at the bloboid $\mathcal{B}_1$: $\mathcal{J}^2 = \mathcal{H}_n, \mathcal{H}_{n-1}, \ldots, \mathcal{H}_1 = \mathcal{B}_1$.

- Form sequence of balloons $\mathcal{B}_1^\star, \ldots, \mathcal{B}_{n-1}^\star$ and pillows $\mathcal{P}_2^\star, \ldots, \mathcal{P}_n^\star$ defining implicitly the sequence of combinatorial 2-complexes $\mathcal{H}_1^\star, \mathcal{H}_1^\star, \ldots, \mathcal{H}_{2n}^\star$, together with their respective wings and nervures (combinatorially given by rotations), $\mathcal{W}_1^\ell \cup \mathcal{N}_1^\ell$, $\mathcal{W}_2^\ell \cup \mathcal{N}_2^\ell$, $\ldots$, $\mathcal{W}_n^\ell \cup \mathcal{N}_n^\ell$ and $\mathcal{W}_1^r \cup \mathcal{N}_1^r$, $\mathcal{W}_2^r \cup \mathcal{N}_2^r$, $\ldots$, $\mathcal{W}_n^r \cup \mathcal{N}_n^r$. Each *bp*-move is simply a flip in the primal sequence. See Figs. 19 to 29 from the r_5^{24}-example.

- Use Tutte's barycentric method with the edge weight heuristic (Fig. 4 from the r_5^{24}-example) to provide rectilinear embeddings of $\mathcal{W}_n^\ell \cup \mathcal{N}_n^\ell$ in Π_ℓ and of $\mathcal{W}_n^r \cup \mathcal{N}_n^r$ in Π_r fixing the outer regions. The nervures are useful up to this point, and after obtaining the rectilinear embeddings they can be discarded.

- Get $\mathcal{H}_1^\diamond$ using $\mathcal{W}_n^\ell \cup \mathcal{W}_n^r$ by the cone construction.

- Get the sequence $\mathcal{H}_2^\diamond, \ldots, \mathcal{H}_n^\diamond = \mathcal{H}_n^\star$ by the blowing up technique in the proof of Theorem 3.1.

- Define the framings of the components of the link as the linking numbers of the boundaries of the cylinders formed by the strips coming from the hinges; special care: distinguish the hinges which become 2-hinges from the hinges which become 3-hinges in M^3. See Fig. 14.

- Find an adequate projection of suitable medial curves in the cylinders. These curves form the link. Find Gauss code for the link, and so, a projection is combinatorially specified ([9], chapter 3 of [5], [8]). Add curls to produce a blackboard framed link. See Figs. 16 and 17 from the r_5^{24}-example.

This algorithm has both space complexity and time complexity $O(n^2)$. Its output, first obtained as a set with no more than n PL-polygons in $\mathbb{R}^3$, has a total of at most $12n^2$ vertices. □

Appendix A: a solution for the Weber-Seifert Dodecahedral Hyperbolic Space

We found a projection for a framed link with 142 crossings for the Weber-Seifert Dodecahedral Hyperbolic Space. Actually the PL-link are nine PL-polygons in $\mathbb{R}^3$ with a total of only 68 vertices. The data that follows is a positive answer for Jeffrey Weeks' question more than twenty years ago. Still in raw form, it can be substantially simplified

We apply our algorithm to the 50-vertex gem and its resolution given at the right side of Fig. 18.

A crossing $x \in \mathbb{N}$ has 4 legs in counterclockwise order: $(4x-3, 4x-2, 4x-1, 4x)$. A *duet* is a perfect matching of the legs. The first entry of a *quintet* is the number of the crossing. Each crossing appears in two consecutive quintets. The second entry is d or u depending on whether the quintet holds the first or the second occurrence of its crossing. The d means that the southwest to the northeast passage goes under, the u means that it goes over. The third and fourth entries of a quintet are legs and their order specifies a consistent orientation for all the components of the link. The fifth and last entry of a quintet is the number of the component of the link that contains the two legs. By properly embedding the quintets in the plane and identifying the legs as specified by the duets we have a link diagram with consistent orientation of all of its component. Thus to obtain a Gauss code ([9], chapter 3 of [5], [8]), for the link is straightforward. Even though there are 142 crossings in the projection, the number of 1-simplices in the PL-link is only 68. This was obtained by a shortcutting technique which started with over two hundred 1-simplices: each 0-simplex defines a triangle in $\mathbb{R}^3$; if this triangle is not pierced by a 1-simplex, then the 0-simplex is removed from the link. Compare 68 with our theoretical bound, namely $12n^2 = 7500$, since $n = 25$. We emphasize the issue that the algorithm behaves very efficiently.

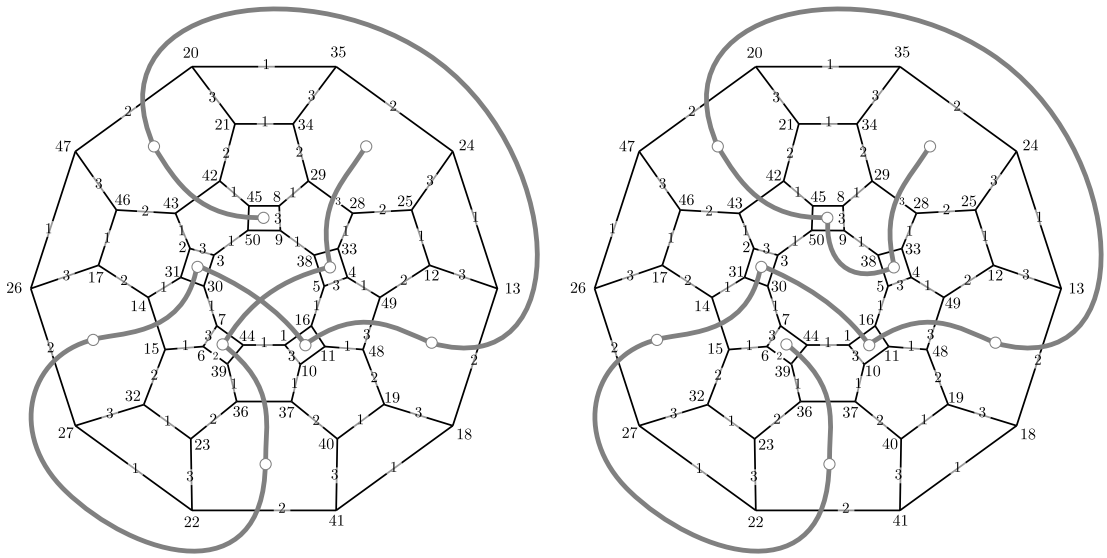

2-twistors: {11, 49}, {15, 31}, {29, 33}, {37, 39}, {43, 45}

3-twistors: {1, 3}, {1,5}, {1, 7}, {1, 9}, {3, 5}, {3, 7}, {3, 9}, {5, 7}, {5, 9}, {7, 9}, {18, 20}, {18, 22}, {18, 24}, {18, 26}, {20, 22}, {20, 24}, {20, 26}, {22, 24}, {22, 26}, {24, 26}

Figure 18: This is a 50-vertex gem which behaves as the *attractor*.

5.1 Duets of $DHIP_{50}^{142}$

1, 8	2, 155	3, 112	4, 111	5, 108	6, 11	7, 104	9, 16
10, 101	12, 107	13, 564	14, 19	15, 102	17, 24	18, 97	20, 159
21, 158	22, 27	23, 468	25, 32	26, 465	28, 163	29, 340	30, 35
31, 336	33, 40	34, 267	36, 271	37, 560	38, 43	39, 268	41, 48
42, 75	44, 559	45, 72	46, 51	47, 76	49, 56	50, 495	52, 71
53, 68	54, 59	55, 188	57, 62	58, 185	60, 63	61, 500	64, 67
65, 70	66, 183	69, 184	73, 494	74, 79	77, 84	78, 263	80, 259
81, 258	82, 85	83, 26	86, 475	87, 92	88, 335	89, 472	90, 93
91, 466	94, 471	95, 98	96, 467	99, 156	100, 103	105, 110	106, 319
109, 320	113, 240	114, 239	115, 526	116, 117	118, 525	119, 122	120, 235
121, 236	123, 142	124, 127	125, 132	126, 531	128, 139	129, 136	130, 135
131, 532	133, 138	134, 317	137, 230	140, 141	143, 146	144, 231	145, 524
147, 528	148, 149	150, 527	151, 154	152, 383	153, 244	157, 164	160, 563
161, 464	162, 167	165, 172	166, 337	168, 463	169, 344	170, 175	171, 338
173, 180	174, 269	176, 275	177, 556	178, 181	179, 558	182, 497	186, 191
187, 496	189, 196	190, 489	192, 427	193, 432	194, 199	195, 488	197, 204
198, 435	200, 431	201, 448	202, 207	203, 544	205, 212	206, 443	208, 447
209, 446	210, 215	211, 538	213, 220	214, 483	216, 371	217, 370	218, 223
219, 376	221, 226	222, 373	224, 311	225, 522	227, 316	228, 229	232, 523
233, 530	234, 237	238, 529	241, 470	242, 247	243, 324	245, 252	246, 321
248, 327	249, 326	250, 253	251, 568	254, 329	255, 260	256, 479	257, 332
261, 334	262, 265	266, 333	270, 557	272, 339	273, 280	274, 553	276, 507
277, 506	278, 283	279, 416	281, 288	282, 413	284, 411	285, 552	286, 291
287, 504	289, 296	290, 295	292, 359	293, 364	294, 299	297, 304	298, 365
300, 363	301, 452	302, 305	303, 366	306, 451	307, 312	308, 369	309, 396
310, 313	314, 395	315, 318	322, 567	323, 392	325, 330	328, 473	331, 476
341, 404	342, 347	343, 408	345, 352	346, 511	348, 403	349, 516	350, 353
351, 512	354, 515	355, 360	356, 551	357, 514	358, 361	362, 519	367, 372
368, 445	374, 379	375, 484	377, 382	378, 535	380, 521	381, 536	384, 387
385, 390	386, 565	388, 391	389, 566	393, 456	394, 399	397, 402	398, 459
400, 455	401, 460	405, 510	406, 409	407, 508	410, 549	412, 505	414, 503
415, 420	417, 502	418, 421	419, 554	422, 501	423, 428	424, 499	425, 430
426, 429	433, 440	434, 485	436, 543	437, 542	438, 441	439, 546	442, 541
444, 537	449, 518	450, 453	454, 517	457, 462	458, 561	461, 562	469, 474
477, 482	478, 533	480, 539	481, 534	486, 545	487, 490	491, 548	492, 493
498, 555	509, 550	513, 520	540, 547				

5.2 Quintets, cylinders and framings of $DHIP_{50}^{142}$

{1, d, 3, 1, 1}	{1, u, 4, 2, 3}	{2, d, 7, 5, 8}	{2, u, 8, 6, 1}	{3, d, 11, 9, 1}	{3, u, 10, 12, 1}
{4, d, 13, 15, 8}	{4, u, 16, 14, 1}	{5, d, 18, 20, 2}	{5, u, 19, 17, 1}	{6, d, 24, 22, 1}	{6, u, 21, 23, 9}
{7, d, 27, 25, 1}	{7, u, 28, 26, 5}	{8, d, 32, 30, 1}	{8, u, 31, 29, 4}	{9, d, 35, 33, 1}	{9, u, 34, 36, 3}
{10, d, 39, 37, 9}	{10, u, 40, 38, 1}	{11, d, 42, 44, 8}	{11, u, 43, 41, 1}	{12, d, 48, 46, 1}	{12, u, 45, 47, 1}
{13, d, 51, 49, 1}	{13, u, 50, 52, 6}	{14, d, 53, 55, 2}	{14, u, 56, 54, 1}	{15, d, 59, 57, 1}	{15, u, 60, 58, 8}
{16, d, 61, 63, 8}	{16, u, 62, 64, 1}	{17, d, 66, 68, 2}	{17, u, 67, 65, 1}	{18, d, 70, 72, 1}	{18, u, 71, 69, 6}
{19, d, 73, 75, 8}	{19, u, 76, 74, 1}	{20, d, 80, 78, 4}	{20, u, 79, 77, 1}	{21, d, 84, 82, 1}	{21, u, 81, 83, 3}
{22, d, 86, 88, 9}	{22, u, 85, 87, 1}	{23, d, 91, 89, 9}	{23, u, 92, 90, 1}	{24, d, 93, 95, 1}	{24, u, 96, 94, 5}
{25, d, 99, 97, 2}	{25, u, 98, 100, 1}	{26, d, 102, 104, 8}	{26, u, 103, 101, 1}	{27, d, 108, 106, 8}	{27, u, 107, 105, 1}
{28, d, 109, 111, 3}	{28, u, 110, 112, 1}	{29, d, 115, 113, 6}	{29, u, 114, 116, 2}	{30, d, 120, 118, 8}	{30, u, 117, 119, 2}
{31, d, 123, 121, 2}	{31, u, 122, 124, 2}	{32, d, 126, 128, 6}	{32, u, 127, 125, 2}	{33, d, 129, 131, 8}	{33, u, 132, 130, 2}
{34, d, 135, 133, 2}	{34, u, 134, 136, 8}	{35, d, 138, 140, 2}	{35, u, 139, 137, 6}	{36, d, 141, 143, 2}	{36, u, 144, 142, 2}
{37, d, 146, 148, 2}	{37, u, 145, 147, 6}	{38, d, 149, 151, 2}	{38, u, 150, 152, 8}	{39, d, 154, 156, 2}	{39, u, 155, 153, 3}
{40, d, 159, 157, 2}	{40, u, 160, 158, 9}	{41, d, 164, 162, 2}	{41, u, 161, 163, 5}	{42, d, 167, 165, 2}	{42, u, 166, 168, 8}
{43, d, 172, 170, 2}	{43, u, 171, 169, 4}	{44, d, 175, 173, 2}	{44, u, 174, 176, 3}	{45, d, 179, 177, 9}	{45, u, 180, 178, 2}
{46, d, 181, 183, 2}	{46, u, 184, 182, 6}	{47, d, 188, 186, 2}	{47, u, 185, 187, 8}	{48, d, 192, 190, 7}	{48, u, 191, 189, 2}
{49, d, 196, 194, 2}	{49, u, 195, 193, 7}	{50, d, 200, 198, 5}	{50, u, 199, 197, 2}	{51, d, 204, 202, 2}	{51, u, 203, 201, 7}
{52, d, 207, 205, 2}	{52, u, 206, 208, 5}	{53, d, 209, 211, 7}	{53, u, 212, 210, 2}	{54, d, 214, 216, 8}	{54, u, 215, 213, 2}
{55, d, 217, 219, 4}	{55, u, 220, 218, 2}	{56, d, 222, 224, 5}	{56, u, 223, 221, 2}	{57, d, 226, 228, 2}	{57, u, 227, 225, 6}
{58, d, 230, 232, 6}	{58, u, 229, 231, 2}	{59, d, 233, 235, 8}	{59, u, 236, 234, 2}	{60, d, 237, 239, 2}	{60, u, 240, 238, 6}
{61, d, 244, 242, 3}	{61, u, 241, 243, 9}	{62, d, 247, 245, 3}	{62, u, 246, 248, 4}	{63, d, 251, 249, 9}	{63, u, 252, 250, 3}
{64, d, 253, 255, 3}	{64, u, 254, 256, 5}	{65, d, 257, 259, 4}	{65, u, 260, 258, 3}	{66, d, 263, 261, 4}	{66, u, 264, 262, 3}
{67, d, 266, 268, 9}	{67, u, 265, 267, 3}	{68, d, 270, 272, 8}	{68, u, 271, 269, 3}	{69, d, 276, 274, 8}	{69, u, 275, 273, 3}
{70, d, 279, 277, 6}	{70, u, 280, 278, 3}	{71, d, 284, 282, 5}	{71, u, 283, 281, 3}	{72, d, 287, 285, 9}	{72, u, 288, 286, 3}
{73, d, 292, 290, 6}	{73, u, 291, 289, 3}	{74, d, 296, 294, 3}	{74, u, 295, 293, 6}	{75, d, 299, 297, 3}	{75, u, 300, 298, 4}
{76, d, 304, 302, 3}	{76, u, 303, 301, 5}	{77, d, 305, 307, 3}	{77, u, 308, 306, 8}	{78, d, 312, 310, 3}	{78, u, 311, 309, 5}
{79, d, 313, 315, 3}	{79, u, 314, 316, 6}	{80, d, 319, 317, 8}	{80, u, 318, 320, 3}	{81, d, 324, 322, 9}	{81, u, 323, 321, 4}
{82, d, 326, 328, 9}	{82, u, 327, 325, 4}	{83, d, 330, 332, 4}	{83, u, 331, 329, 5}	{84, d, 335, 333, 9}	{84, u, 334, 336, 4}
{85, d, 339, 337, 8}	{85, u, 340, 338, 4}	{86, d, 344, 342, 4}	{86, u, 341, 343, 5}	{87, d, 347, 345, 4}	{87, u, 346, 348, 9}
{88, d, 351, 349, 6}	{88, u, 352, 350, 4}	{89, d, 353, 355, 4}	{89, u, 354, 356, 8}	{90, d, 357, 359, 6}	{90, u, 360, 358, 4}
{91, d, 364, 362, 6}	{91, u, 361, 363, 4}	{92, d, 365, 367, 4}	{92, u, 368, 366, 5}	{93, d, 372, 370, 4}	{93, u, 371, 369, 8}
{94, d, 376, 374, 4}	{94, u, 375, 373, 5}	{95, d, 379, 377, 4}	{95, u, 380, 378, 6}	{96, d, 382, 384, 4}	{96, u, 383, 381, 8}
{97, d, 387, 385, 4}	{97, u, 386, 388, 9}	{98, d, 391, 389, 9}	{98, u, 390, 392, 4}	{99, d, 393, 395, 6}	{99, u, 396, 394, 5}
{100, d, 399, 397, 5}	{100, u, 400, 398, 5}	{101, d, 403, 401, 9}	{101, u, 402, 404, 5}	{102, d, 407, 405, 6}	{102, u, 408, 406, 5}
{103, d, 410, 412, 8}	{103, u, 409, 411, 5}	{104, d, 414, 416, 6}	{104, u, 413, 415, 5}	{105, d, 419, 417, 9}	{105, u, 420, 418, 5}
{106, d, 421, 423, 5}	{106, u, 424, 422, 6}	{107, d, 425, 427, 7}	{107, u, 428, 426, 5}	{108, d, 429, 431, 5}	{108, u, 432, 430, 7}
{109, d, 435, 433, 5}	{109, u, 436, 434, 6}	{110, d, 439, 437, 7}	{110, u, 440, 438, 5}	{111, d, 441, 443, 5}	{111, u, 444, 442, 6}
{112, d, 448, 446, 7}	{112, u, 447, 445, 5}	{113, d, 451, 449, 8}	{113, u, 452, 450, 5}	{114, d, 454, 456, 6}	{114, u, 453, 455, 5}
{115, d, 460, 458, 9}	{115, u, 459, 457, 5}	{116, d, 463, 461, 8}	{116, u, 462, 464, 5}	{117, d, 468, 466, 9}	{117, u, 465, 467, 5}
{118, d, 472, 470, 9}	{118, u, 471, 469, 5}	{119, d, 473, 475, 9}	{119, u, 474, 476, 5}	{120, d, 479, 477, 5}	{120, u, 478, 480, 6}
{121, d, 482, 484, 5}	{121, u, 481, 483, 8}	{122, d, 486, 488, 7}	{122, u, 485, 487, 6}	{123, d, 489, 491, 7}	{123, u, 490, 492, 6}
{124, d, 496, 494, 8}	{124, u, 493, 495, 6}	{125, d, 498, 500, 8}	{125, u, 497, 499, 6}	{126, d, 501, 503, 6}	{126, u, 502, 504, 9}
{127, d, 506, 508, 6}	{127, u, 505, 507, 8}	{128, d, 510, 512, 6}	{128, u, 509, 511, 9}	{129, d, 516, 514, 6}	{129, u, 513, 515, 8}
{130, d, 519, 517, 6}	{130, u, 518, 520, 8}	{131, d, 523, 521, 6}	{131, u, 522, 524, 6}	{132, d, 525, 527, 8}	{132, u, 528, 526, 6}
{133, d, 532, 530, 8}	{133, u, 529, 531, 6}	{134, d, 536, 534, 8}	{134, u, 535, 533, 6}	{135, d, 538, 540, 7}	{135, u, 539, 537, 6}
{136, d, 542, 544, 7}	{136, u, 541, 543, 6}	{137, d, 548, 546, 7}	{137, u, 547, 545, 7}	{138, d, 551, 549, 8}	{138, u, 552, 550, 9}
{139, d, 556, 554, 9}	{139, u, 553, 555, 8}	{140, d, 560, 558, 9}	{140, u, 559, 557, 8}	{141, d, 562, 564, 8}	{141, u, 561, 563, 9}
{142, d, 566, 568, 9}	{142, u, 567, 565, 9}				

framed component (thin cylinder)	i-twistor	linking number of cylinder component
1	$2-\{19,13\}$	-1
2	$2-\{3,29\}$	0
3	$2-\{49,33\}$	-1
4	$2-\{39,43\}$	-1
5	$2-\{9,23\}$	-2
6	$3-\{1,31\}$	0
7	$3-\{6,26\}$	0
8	$3-\{46,36\}$	0
9	$3-\{11,21\}$	0

Appendix B: all figures for the r_5^{24}-example. This produces an overview of the data structure and their interrelations illustrating the general case of the algorithm

In the following figures, the notation $\nabla_{v,i+1}$, $i \geq 1$, denotes the PL3-face dual of the vertex v of the input gem obtained after the i-th *bp*-move is performed. If after the i-th *bp*-move $\nabla_{v,i}$ does not change, then $\nabla_{v,i+1} = \nabla_{v,i}$. When there is a change, it is an ϵ-change.

References

[1] É. Colin de Verdière, M. Pocchiola, and G. Vegter. Tutte's barycenter method applied to isotopies. *Computational Geometry*, 26(1):81–97, 2003.

[2] E Klarreich. Network solutions. *Simons Foundation*, April, 2012.

[3] W.B.R. Lickorish. *An introduction to knot theory*, volume 175. Springer Verlag, 1997.

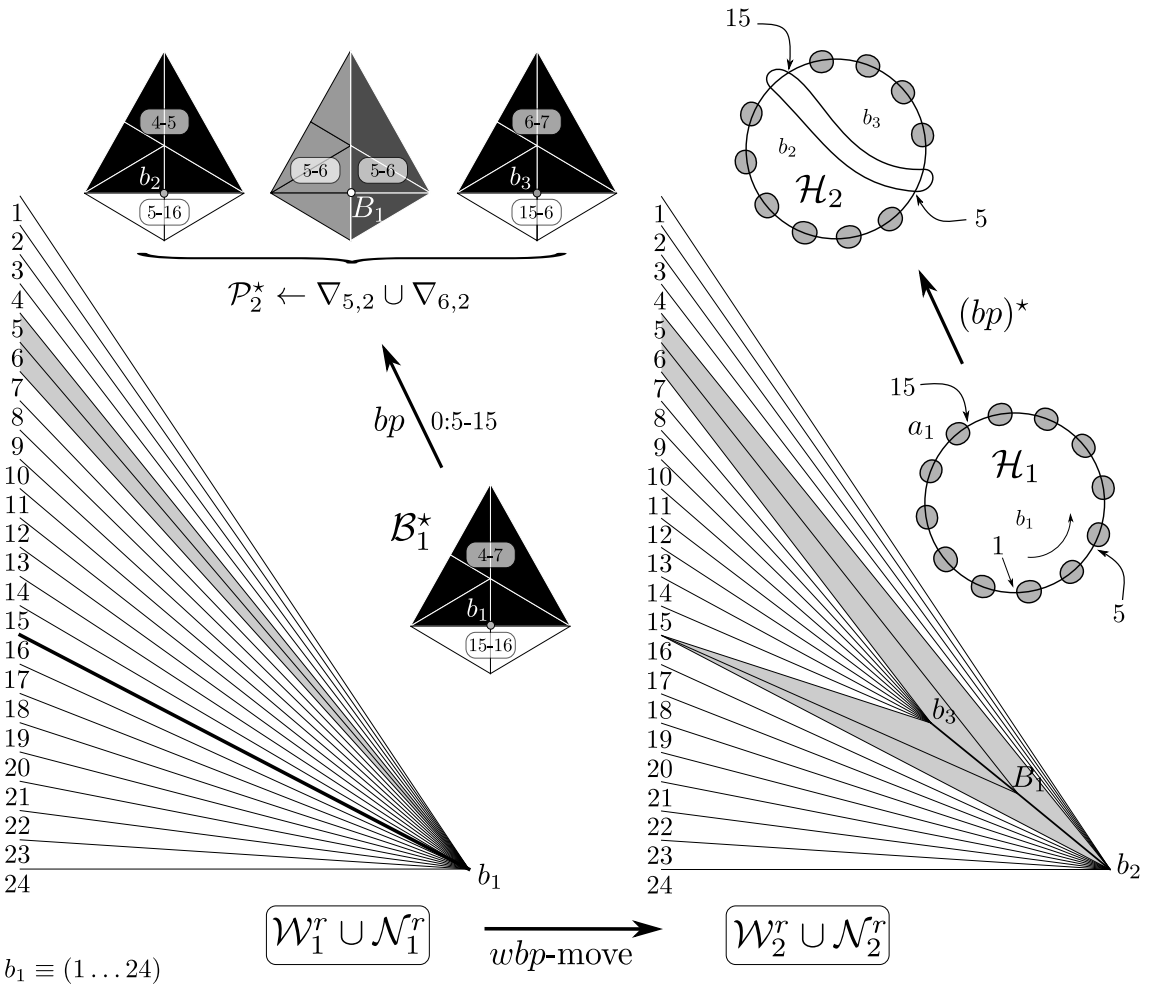

Figure 19: $\mathcal{H}_2^\star \leftarrow \mathcal{H}_1^\star \cup (\mathcal{P}_2^\star \backslash \mathcal{B}_1^\star)$. Pillow $\mathcal{P}_2^\star \leftarrow \nabla_{5,12} \cup \nabla_{6,12}$ (r_5^{24}-example).

[4] L.D. Lins. Blink: a language to view, recognize, classify and manipulate 3d-spaces. *Arxiv preprint math/0702057*, 2007.

[5] S. Lins. *Graphs of maps, Available in the arXiv as math.CO/0305058*. PhD thesis, University of Waterloo, 1980.

[6] S. Lins and R. Machado. Framed link presentations of 3-manifolds by an $O(n^2)$ algorithm, I: gems and their duals. *arXiv:1211.1953v2 [math.GT]*, 2012.

[7] S. Lins and R. Machado. Framed link presentations of 3-manifolds by an $O(n^2)$ algorithm, II: colored complexes and boundings in their complexity. *arXiv:1212.0826v2 [math.GT]*, 2012.

[8] S. Lins, E. Oliveira-Lima, and V. Silva. A homological solution for the Gauss code problem in arbitrary surfaces. *Journal of Combinatorial Theory, Series B*, 98(3):506–515, 2008.

[9] P. Rosenstiehl. Solution algebrique du probleme de Gauss sur la permutation des points d'intersection d'une ou plusieurs courbes fermees du plan. *CR Acad. Sci.*, 283:551–553, 1976.

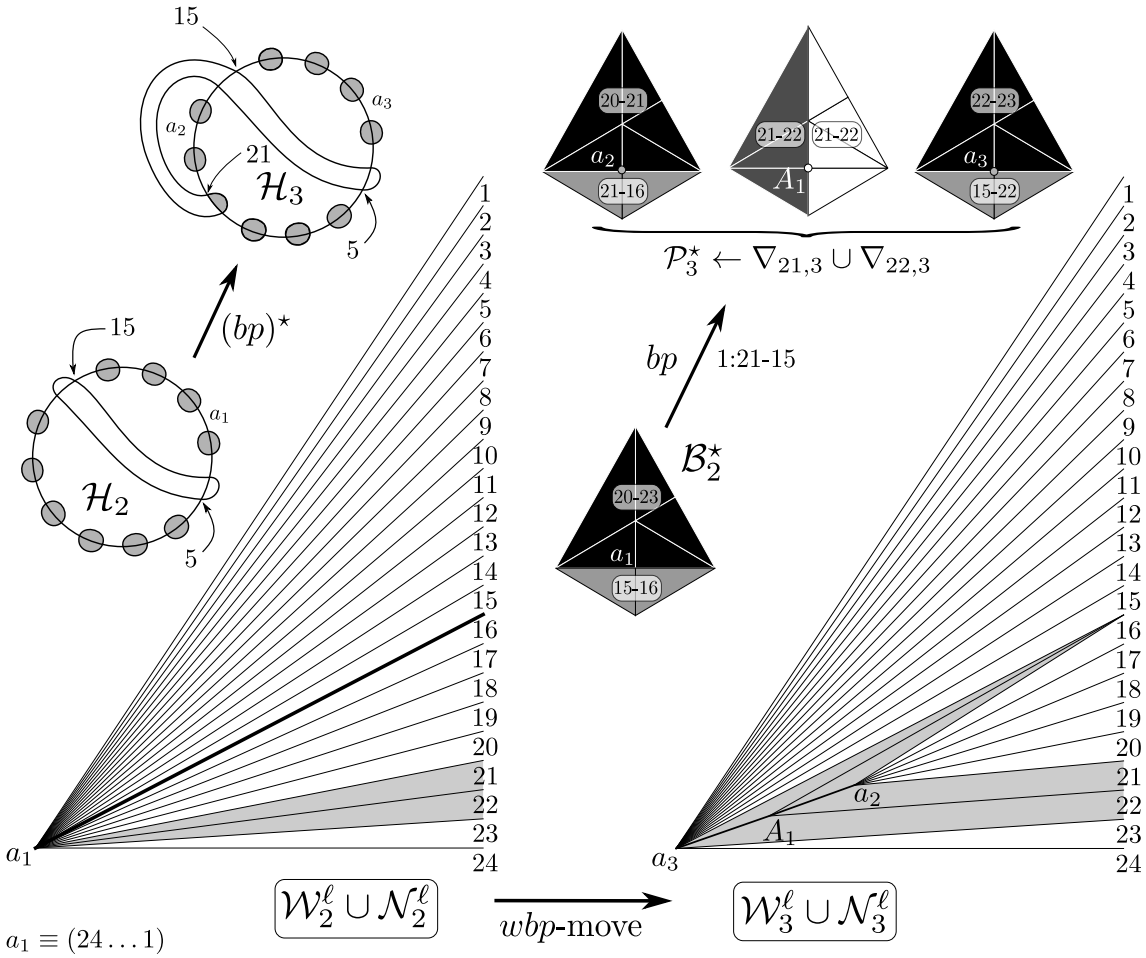

$a_1 \equiv (24 \dots 1)$

13-gon a_1 is subdivided into a_2 and a_3

$u(2) = 21, v(2) = 22, r(2) = 15, s(2) = 16, c(2) = 1$

$t_a(2) = 1, \ell_a(2) = 1, \ell_a(3) = 3$

$a_2 \equiv (21, 20, 19, 18, 17, 16)$

$a_3 \equiv (15, 14, 13, 12, 11, 10, 9, 8, 7, 6, 5, 4, 3, 2, 1, 24, 23, 22)$

Figure 20: $\mathcal{H}_3^\star \leftarrow \mathcal{H}_2^\star \cup (\mathcal{P}_3^\star \backslash \mathcal{B}_2^\star)$. Pillow $\mathcal{P}_3^\star \leftarrow \nabla_{21,12} \cup \nabla_{22,12}$ (r_5^{24}-example).

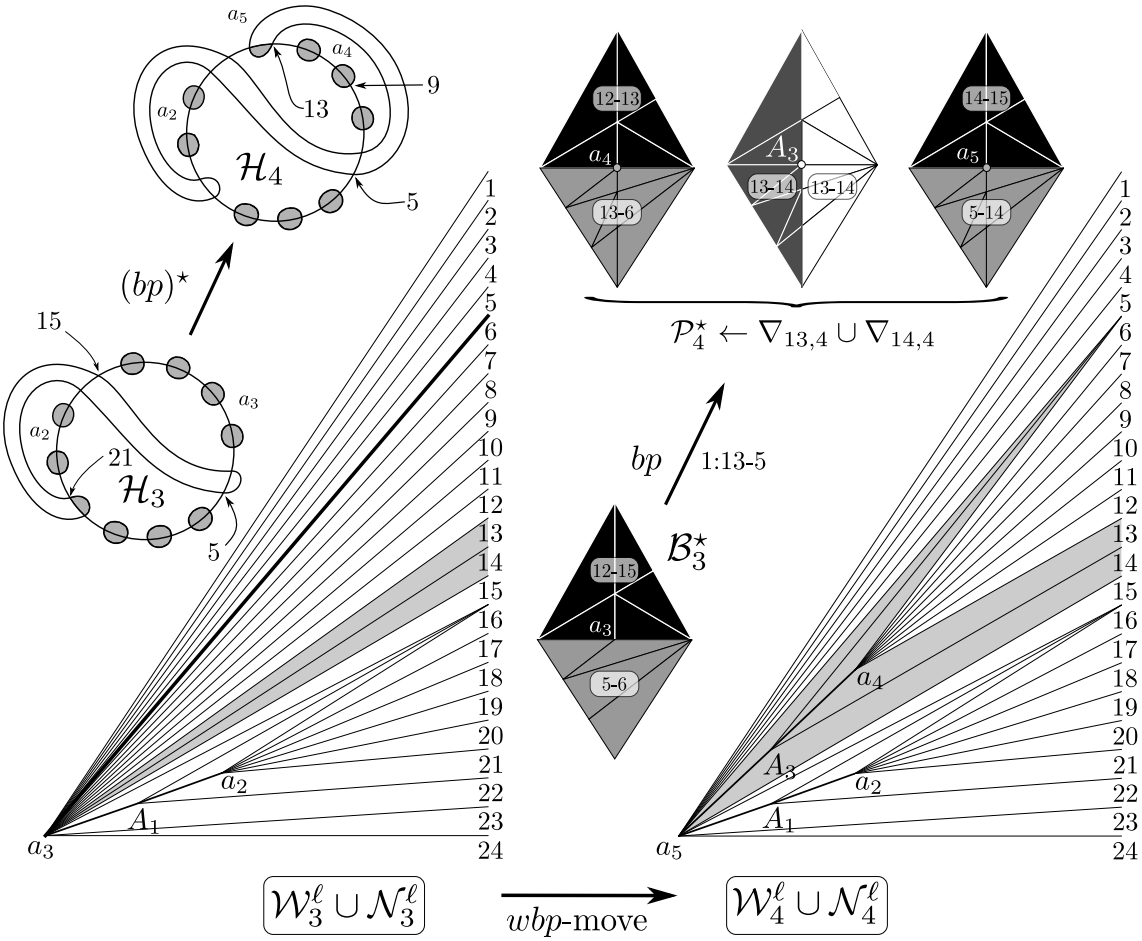

13-gon a_3 is subdivided into a_4 and a_5

$u(3) = 13, v(3) = 14, r(3) = 5, s(3) = 6, c(3) = 1$

$t_a(3) = 3, \ell_a(3) = 3, \ell_a(4) = 5$

$a_2 \equiv (21, 20, 19, 18, 17, 16)$ $a_4 \equiv (13, 12, 11, 10, 9, 8, 7, 6)$ $a_5 \equiv (15, 14, 5, 4, 3, 2, 1, 24, 23, 22)$

Figure 21: $\mathcal{H}_4^\star \leftarrow \mathcal{H}_3^\star \cup (\mathcal{P}_4^\star \backslash \mathcal{B}_3^\star)$. Pillow $\mathcal{P}_4^\star \leftarrow \nabla_{13,12} \cup \nabla_{14,12}$ (r_5^{24}-example).

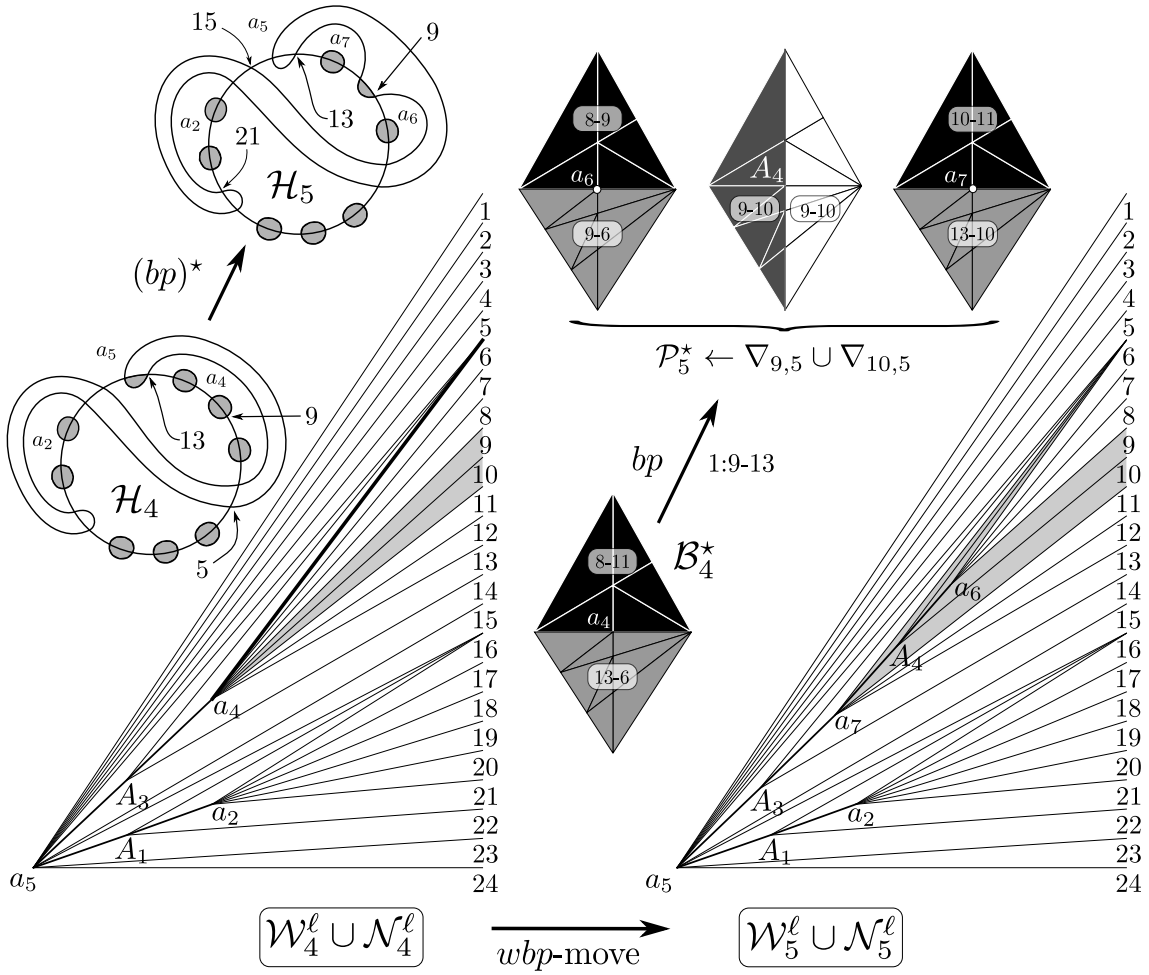

13-gon a_4 is subdivided into a_6 and a_7

$u(4) = 9, v(4) = 10, r(4) = 13, s(4) = 6, c(4) = 1$

$t_a(4) = 4, \ell_a(4) = 5, \ell_a(5) = 7$

$a_2 \equiv (21, 20, 19, 18, 17, 16)$ $a_5 \equiv (15, 14, 5, 4, 3, 2, 1, 24, 23, 22)$ $a_6 \equiv (9, 8, 7, 6)$ $a_7 \equiv (13, 12, 11, 10)$

Figure 22: $\mathcal{H}_5^\star \leftarrow \mathcal{H}_4^\star \cup (\mathcal{P}_5^\star \backslash \mathcal{B}_4^\star)$. Pillow $\mathcal{P}_5^\star \leftarrow \nabla_{9,12} \cup \nabla_{10,12}$ (r_5^{24}-example).

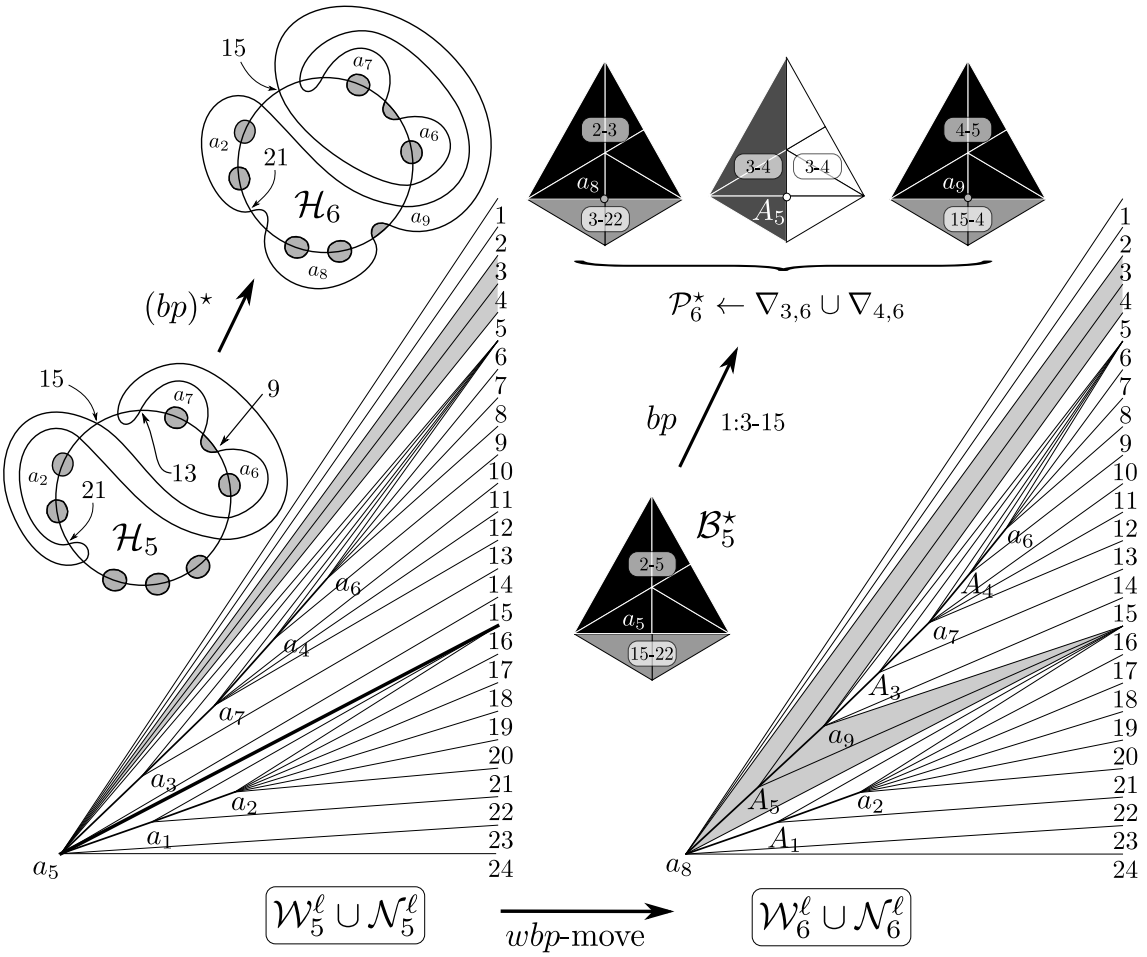

13-gon a_5 is subdivided into a_8 and a_9

$u(5) = 3, v(5) = 4, r(5) = 15, s(5) = 22, c(5) = 1$

$t_a(5) = 5, \ell_a(5) = 7, \ell_a(6) = 9$

$a_2 \equiv (21, 20, 19, 18, 17, 16)$ $a_6 \equiv (9, 8, 7, 6)$ $a_7 \equiv (13, 12, 11, 10)$ $a_8 \equiv (3, 2, 1, 24, 23, 22)$

$a_9 \equiv (15, 14, 5, 4)$

Figure 23: $\mathcal{H}_6^\star \leftarrow \mathcal{H}_5^\star \cup (\mathcal{P}_6^\star \backslash \mathcal{B}_5^\star)$. Pillow $\mathcal{P}_6^\star \leftarrow \nabla_{3,12} \cup \nabla_{4,12}$ (r_5^{24}-example).

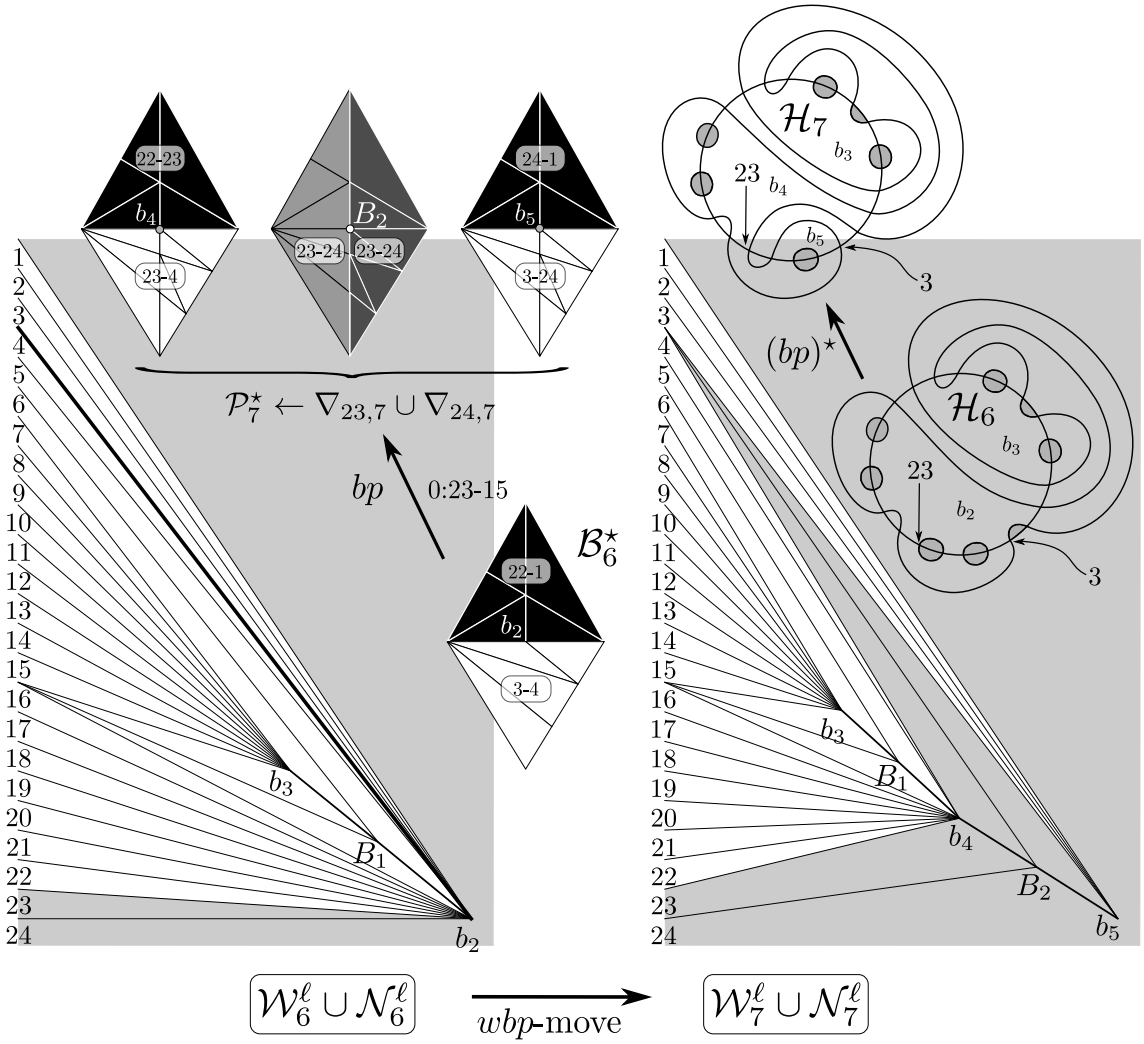

03-gon b_2 is subdivided into b_4 and b_5

$u(6) = 23, v(6) = 24, r(6) = 3, s(6) = 4, c(6) = 0$

$t_b(6) = 2, \ell_b(6) = 3, \ell_b(7) = 5$

$b_3 \equiv (15, 6, 7, 8, 9, 10, 11, 12, 13, 14)$ $b_4 \equiv (5, 16, 17, 18, 19, 20, 21, 22, 23, 4)$ $b_5 \equiv (24, 1, 2, 3)$

Figure 24: $\mathcal{H}_7^\star \leftarrow \mathcal{H}_6^\star \cup (\mathcal{P}_7^\star \backslash \mathcal{B}_6^\star)$. Pillow $\mathcal{P}_7^\star \leftarrow \nabla_{23,12} \cup \nabla_{24,12}$ (r_5^{24}-example).

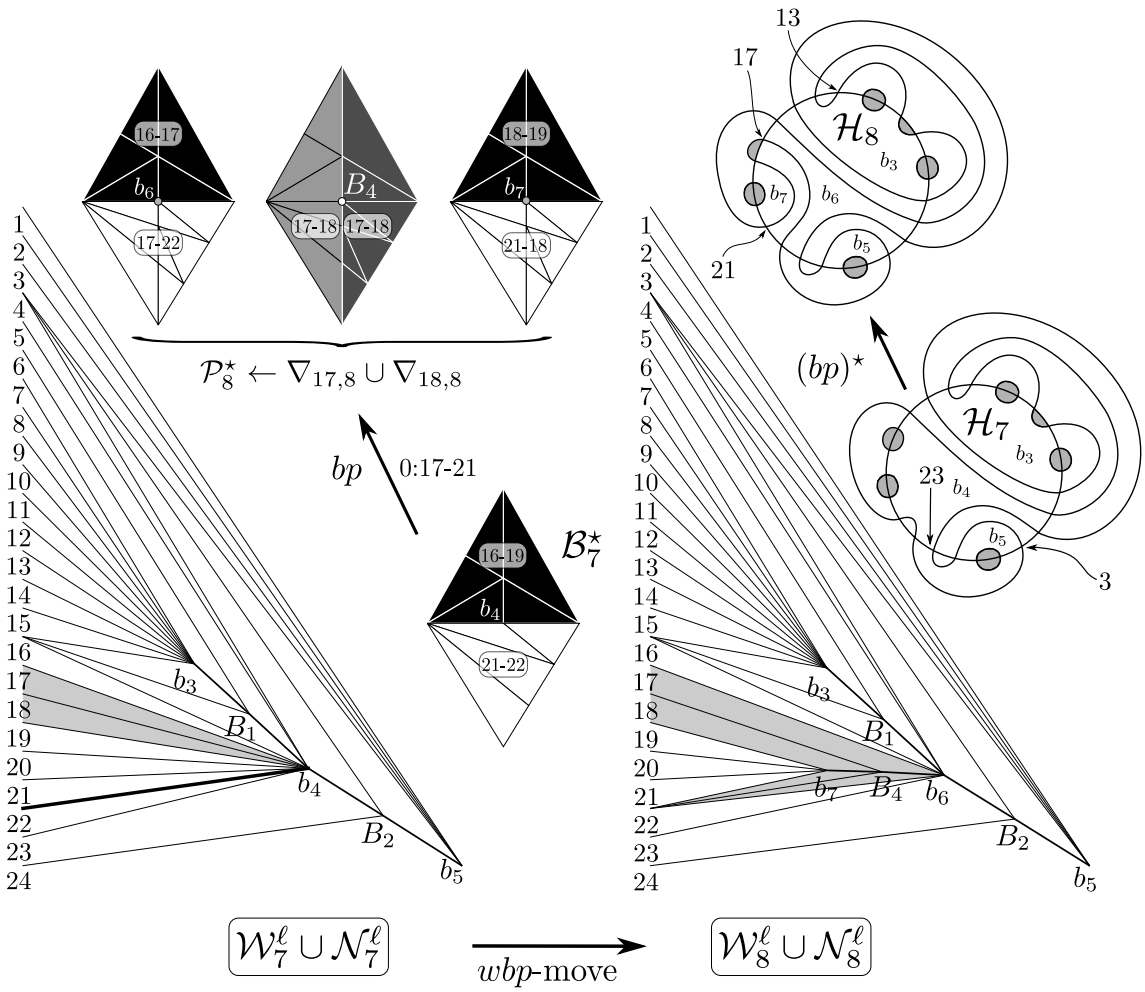

03-gon b_4 is subdivided into b_6 and b_7

$u(7) = 17, v(7) = 18, r(7) = 21, s(7) = 22, c(7) = 0$

$t_b(7) = 4, \ell_b(7) = 5, \ell_b(8) = 7$

$b_3 \equiv (15, 6, 7, 8, 9, 10, 11, 12, 13, 14)$ $b_5 \equiv (24, 1, 2, 3)$ $b_6 \equiv (5, 16, 17, 22, 23, 4)$ $b_7 \equiv (18, 19, 20, 21)$

Figure 25: $\mathcal{H}_8^\star \leftarrow \mathcal{H}_7^\star \cup (\mathcal{P}_8^\star \backslash \mathcal{B}_7^\star)$. Pillow $\mathcal{P}_8^\star \leftarrow \nabla_{17,12} \cup \nabla_{18,12}$ (r_5^{24}-example).

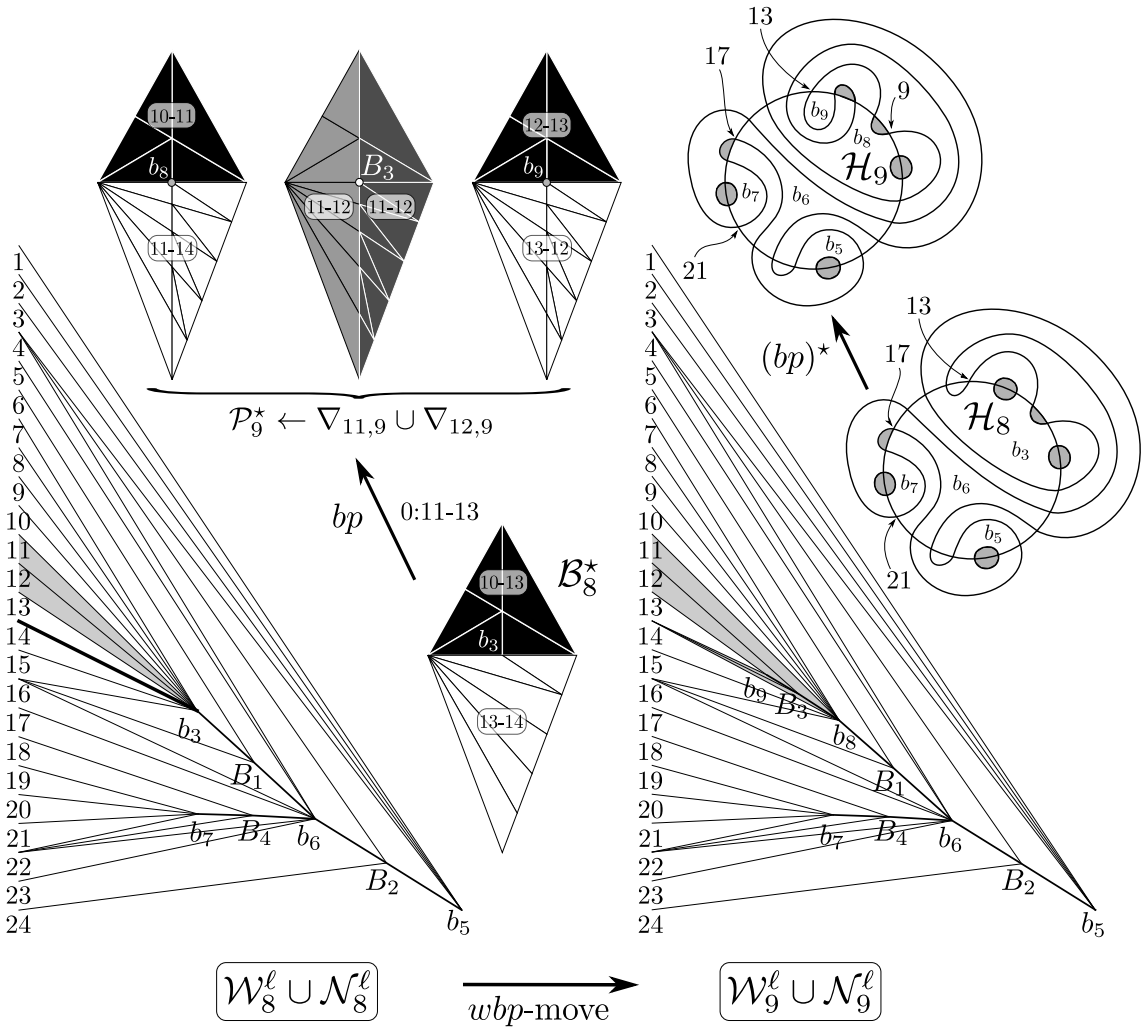

03-gon b_3 is subdivided into b_8 and b_9

$u(8) = 11, v(8) = 12, r(8) = 13, s(8) = 14, c(8) = 0$

$t_b(8) = 3, \ell_b(8) = 7, \ell_b(9) = 9$

$b_5 \equiv (24, 1, 2, 3)$ $b_6 \equiv (5, 16, 17, 22, 23, 4)$ $b_7 \equiv (18, 19, 20, 21)$ $b_8 \equiv (15, 6, 7, 8, 9, 10, 11, 14)$
$b_9 \equiv (12, 13)$

Figure 26: $\mathcal{H}_9^\star \leftarrow \mathcal{H}_8^\star \cup (\mathcal{P}_9^\star \backslash \mathcal{B}_8^\star)$. Pillow $\mathcal{P}_9^\star \leftarrow \nabla_{11,12} \cup \nabla_{12,12}$ (r_5^{24}-example).

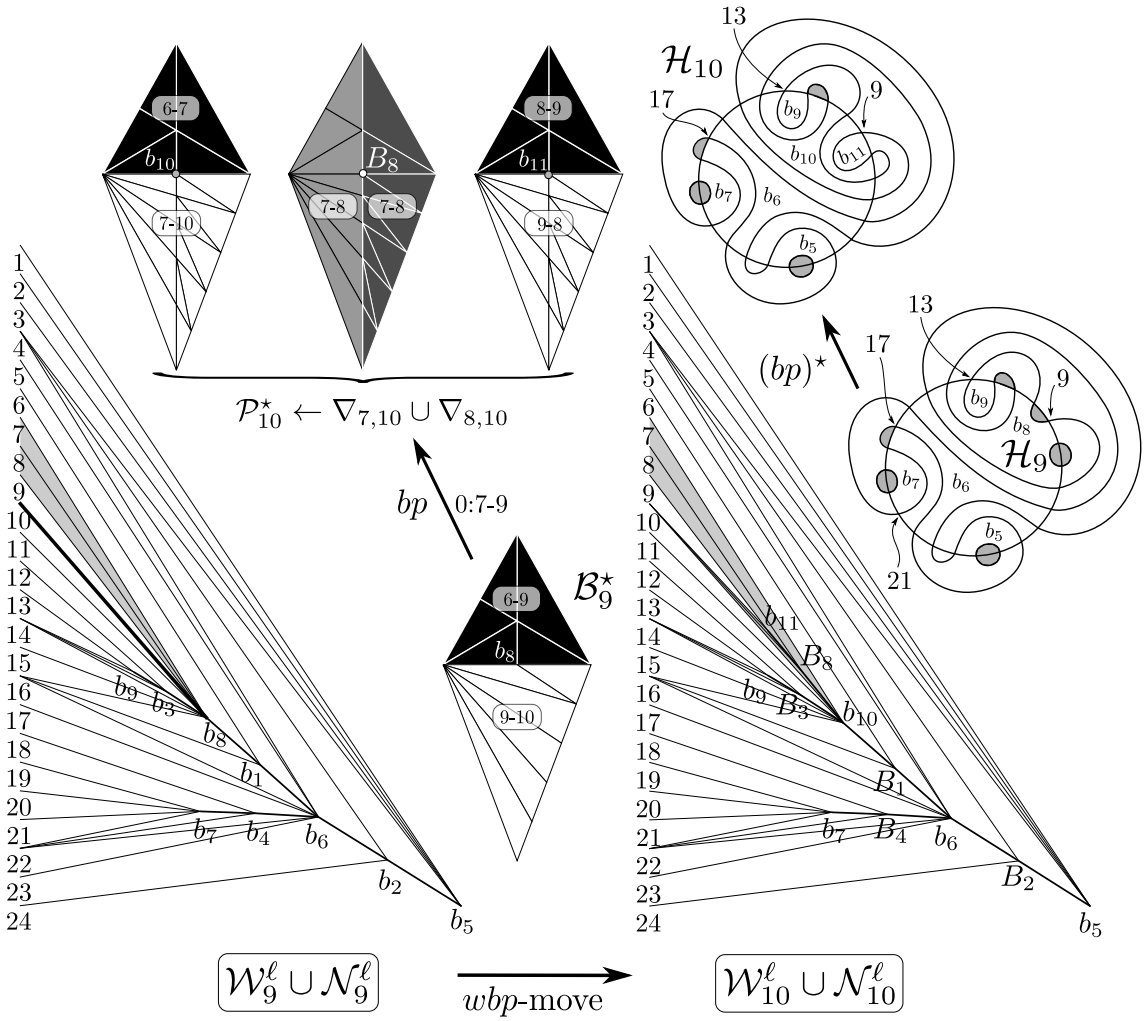

03-gon b_8 is subdivided into b_{10} and b_{11}

$u(9) = 7, v(9) = 8, r(9) = 9, s(9) = 10, c(9) = 0$

$t_b(9) = 8, \ell_b(9) = 9, \ell_b(10) = 11$

$b_5 \equiv (24, 1, 2, 3)$ $b_6 \equiv (5, 16, 17, 22, 23, 4)$ $b_7 \equiv (18, 19, 20, 21)$ $b_9 \equiv (12, 13)$

$b_{10} \equiv (15, 6, 7, 10, 11, 14)$ $b_{11} \equiv (8, 9)$

Figure 27: $\mathcal{H}^\star_{10} \leftarrow \mathcal{H}^\star_9 \cup (\mathcal{P}^\star_{10} \backslash \mathcal{B}^\star_9)$. Pillow $\mathcal{P}^\star_{10} \leftarrow \nabla_{7,12} \cup \nabla_{8,12}$ (r^{24}_5-example).

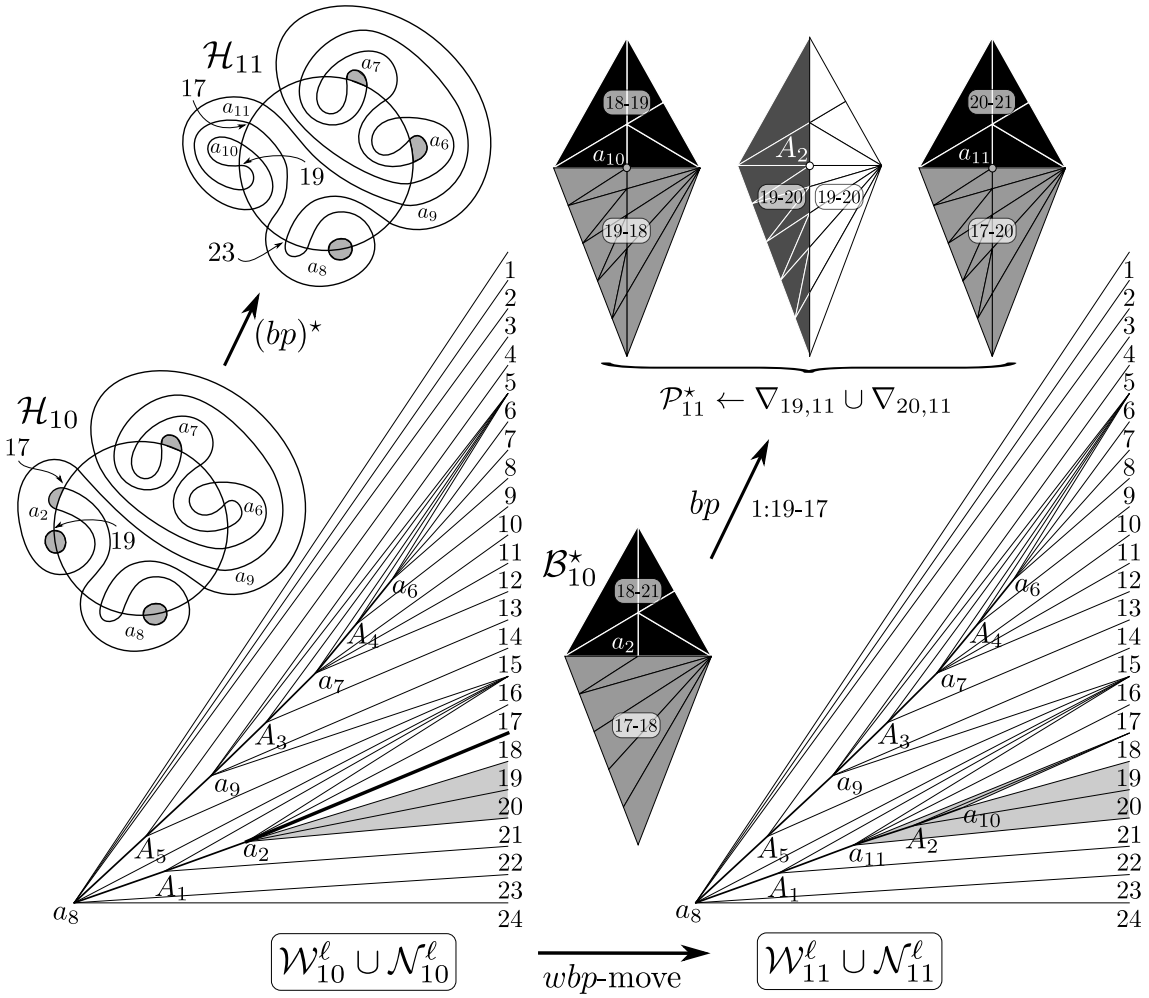

13-gon a_2 is subdivided into a_{10} and a_{11}

$u(10) = 19, v(10) = 20, r(10) = 17, s(10) = 18, c(10) = 1$

$t_a(10) = 2, \ell_a(10) = 9, \ell_a(11) = 11$

$a_6 \equiv (9, 8, 7, 6)$ $a_7 \equiv (13, 12, 11, 10)$ $a_8 \equiv (3, 2, 1, 24, 23, 22)$ $a_9 \equiv (15, 14, 5, 4)$ $a_{10} \equiv (19, 18)$ $a_{11} \equiv (21, 20, 17, 16)$

Figure 28: $\mathcal{H}^\star_{11} \leftarrow \mathcal{H}^\star_{10} \cup (\mathcal{P}^\star_{11} \backslash \mathcal{B}^\star_{10})$. Pillow $\mathcal{P}^\star_{11} \leftarrow \nabla_{19,12} \cup \nabla_{20,12}$ (r^{24}_5-example).

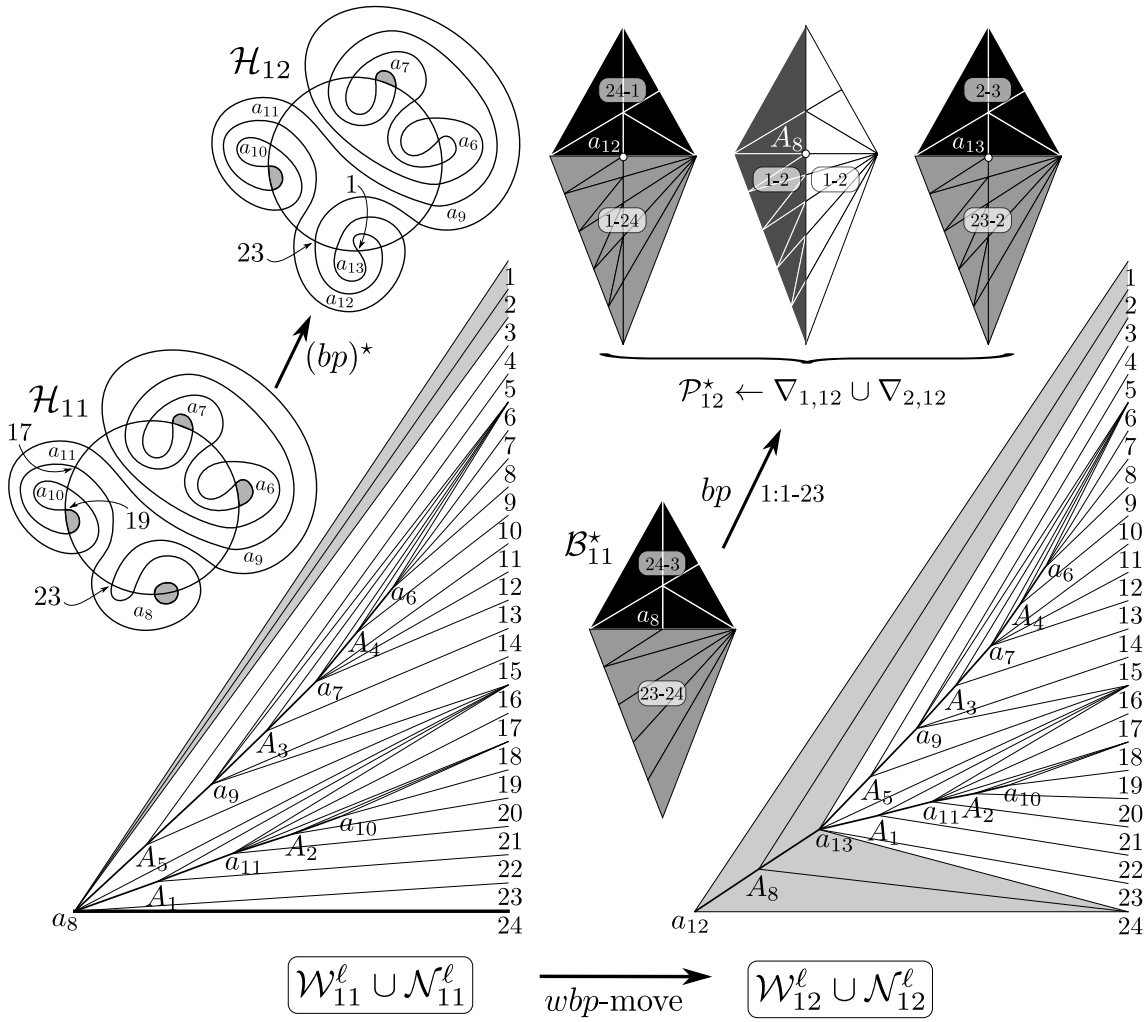

13-gon a_8 is subdivided into a_{12} and a_{13}

$u(11) = 1, v(11) = 2, r(11) = 23, s(11) = 24, c(11) = 1$

$t_a(11) = 8, \ell_a(11) = 1$

$a_6 \equiv (9, 8, 7, 6)$ $a_7 \equiv (13, 12, 11, 10)$ $a_9 \equiv (15, 14, 5, 4)$ $a_{10} \equiv (19, 18)$ $a_{11} \equiv (21, 20, 17, 16)$
$a_{12} \equiv (3, 2, 23, 22)$ $a_{13} \equiv (1, 24)$

Figure 29: $\mathcal{H}^\star_{12} \leftarrow \mathcal{H}^\star_{11} \cup (\mathcal{P}^\star_{12} \backslash \mathcal{B}^\star_{11})$. Pillow $\mathcal{P}^\star_{12} \leftarrow \nabla_{1,12} \cup \nabla_{2,12}$ (r^{24}_5-example).

[10] C.P. Rourke and B.J. Sanderson. *Introduction to piecewise-linear topology*, volume 69. Springer-Verlag, 1982.

[11] W.T. Tutte. How to draw a graph. *Proc. London Math. Soc*, 13(3):743–768, 1963.

Sóstenes L. Lins
Centro de Informática, UFPE
Recife–PE
Brazil
sostenes@cin.ufpe.br

Ricardo N. Machado
Núcleo de Formação de Docentes, UFPE
Caruaru–PE
Brazil
ricardonmachado@gmail.com